Climate Dynamics (2020) 54:1913–1935
https://doi.org/10.1007/s00382-019-05094-4

Impact of Arctic amplification on declining spring dust events in East Asia

Jun Liu[1] · Dongyou Wu[1] · Guangjing Liu[1] · Rui Mao[2] · Siyu Chen[1] · Mingxia Ji[1] · Pingqing Fu[3] · Yele Sun[4] · Xiaole Pan[4] · Hongchun Jin[5] · Yubin Zhou[6] · Xin Wang[1,3]

Received: 21 February 2019 / Accepted: 13 December 2019 / Published online: 26 December 2019

Abstract

Dust aerosols play key roles in affecting regional and global climate through their direct, indirect, and semi-direct effects. Dust events have decreased rapidly since the 1980s in East Asia, particularly over northern China, primarily because of changes in meteorological parameters (e.g. surface wind speed and precipitation). In this study, we found that winter (December–January–February) Arctic amplification associated with weakened temperature gradients along with decreased zonal winds is primarily responsible for the large decline in following spring (March–April–May) dust event occurrences over northern China since the mid-1980s. A dust index was developed for northern China by combining the daily frequency of three types of dust event (dust storm, blowing dust, and floating dust). Using the empirical orthogonal function (EOF) analysis, the first pattern of dust events was obtained for spring dust index anomalies, which accounts for 56.2% of the variability during 1961–2014. Moreover, the enhanced Arctic amplification and stronger Northern Hemisphere annular mode (NAM) in winter can result in the anticyclonic anomalies over Siberia and Mongolia, while cyclonic anomalies over East Europe in spring. These results are significantly correlated with the weakened temperature gradients, increased precipitation and soil moisture, and decreased snow cover extent in the mid-latitude over Northern Hemisphere. Based on the future predictions obtained from the Fifth Climate Models Intercomparison Project (CMIP5), we found that the dust event occurrences may continually decrease over northern China due to the enhanced Arctic amplification in future climate.

Keywords Dust event occurrences · Dust index · Arctic amplification · Temperature gradient · Future prediction

1 Introduction

Dust aerosols emitted into the atmosphere can affect the climate system directly by modifying the radiation budget (Sokolik and Toon 1996; Huang et al. 2006; Fu et al. 2009), indirectly by altering cloud microphysical properties (Twomey et al. 1984; Ackerman et al. 2000; Sassen et al. 2003; Andreae and Rosenfeld 2008; Wang et al. 2010), and possibly by suppressing rainfall processes (Rosenfeld et al. 2001; Solmon et al. 2008; Creamean et al. 2013). Dust can be transported thousands of kilometers from source regions to downwelling areas (Duce et al. 1980; Hsu et al. 2012; Huang et al. 2015; Guo et al. 2017; Chen et al. 2018; Ma et al. 2019). Once large amounts of dust aerosols are deposited into the oceans, soluble or bioavailable iron from dust aerosols can affect biogeochemical processes in the ocean (Jickells et al. 2005). On a regional scale, radiative forcing by dust aerosols can greatly exceed that due to sulfate aerosols and can be comparable to that of clouds, which may

✉ Xin Wang
wxin@lzu.edu.cn

1 Key Laboratory for Semi-Arid Climate Change of the Ministry of Education, College of Atmospheric Sciences, Lanzhou University, Lanzhou 730000, China

2 State Key Laboratory of Earth Surface Processes and Resource Ecology, Beijing Normal University, Beijing 100875, China

3 Institute of Surface-Earth System Science, Tianjin University, Tianjin 300072, China

4 State Key Laboratory of Atmospheric Boundary Layer Physics and Atmospheric Chemistry, Institute of Atmospheric Physics, Chinese Academy of Sciences, Beijing 100029, China

5 KuWeather Science and Technology, Haidian, Beijing 100085, China

6 National Deep Sea Center, Qingdao, Shandong, China

adversely affect the water supply by effecting on the temperature, along with the role of aerosols as cloud condensation nuclei (Sokolik and Toon 1996; Kaufman et al. 2002). Up to now, the radiative forcing and optical properties of dust aerosols have been thoroughly investigated using multi-satellite retrievals (Kaufman et al. 2002; Jin et al. 2014, 2015), and ground-based instruments measurements (Huebert et al. 2003; Li et al. 2010; Wang et al. 2010, 2015a, b, 2018b; Pu et al. 2015; Che et al. 2015, 2019; Chen et al. 2018; Wu et al. 2018b). In addition, the long-term variations in the dust event occurrences related to the meteorological factors and global climate have been extensively analyzed based on observations (Chiapello et al. 2005; Hara et al. 2006; Fan et al. 2017; Ji and Fan 2019) and model simulations (Ginoux et al. 2004; Mukai et al. 2004; Mao et al. 2011b).

Dust aerosols primarily originate from dust source regions over the globe. Recently, East Asia and surrounding areas, which contain several dust source regions, have been the focus of much scientific attention. Dust aerosols emitted from the Gobi Desert and Taklimakan Desert along with the adjacent dust source regions over northern China account for 70% of the total dust emissions in Asia (Zhang et al. 2003). Variations in dust activity in East Asia (e.g., dust events and dust transport) are believed to be associated with changes in large-scale atmospheric circulation (Husar et al. 1997; Gong et al. 2006a), surface wind (Kurosaki and Mikami 2003; Wang et al. 2018a), cyclone frequency (Qian et al. 2002; Zhu et al. 2008), the intensity of the East Asian monsoon (Wu et al. 2010), Northern Hemisphere annular mode (NAM) (Yin et al. 2013; Li et al. 2019), or Arctic Oscillation (AO) (Mao et al. 2011a, b). Changes in atmospheric circulation associated with sand-driving mechanisms are main causes in the reduction of dust events. Good correspondence was found between the surface wind speed and dust occurrences (Kurosaki and Mikami 2003; Zhao et al. 2004). A steady decrease in zonal maximum wind speed (up to -0.95 m/s) is largely responsible for the decline in dust event occurrences over northern China since the beginning of this century (Wang et al. 2018a). Previous researches exhibited that an enhanced geopotential height over the Mongolian Plateau and an increase in precipitation over northwest China (Ding et al. 2005), along with the reduced cyclone frequency over northern China (Qian et al. 2002) and Mongolia (Zhu et al. 2008) are closely correlated with the reduction of dust events. Moreover, the decline in dust events also interacts with large scale climate fields. Researches indicated that the spring dust occurrences exhibit an increase during negative phases of the AO, by contributing to atmospheric instability (Gong et al. 2006a; Lee et al. 2014). Besides the AO, interannual variations of the Antarctic Oscillation (AAO) play a significant role in dust-related atmospheric circulation during boreal spring (Fan and Wang 2004). Ji and Fan (2019) further showed that positive AAO in winter provides dynamical conditions, which are conducive to reducing dust weather frequency over northern China by affecting atmospheric circulation changes. Furthermore, indirect effect of the ocean process (e.g. the interdecadal variability and sea ice retreat) can't be ignored. Gong et al. (2006b) showed that there are fewer dust aerosols in East Asia during the warm phase of the Pacific decadal oscillation (PDO), because of air-sea interactions between the global westerly belt and sea surface temperature (SST) in the North Pacific. In negative AO phase years, frequency of dust events shows a significant increase in the years of El Niño compared with those in the years of La Niña (Lee et al. 2014). Moreover, Fan et al. (2017) found that decreased winter sea ice cover in the Barents Sea leads to an increased frequency of dust events during the period of 1996–2014 over North China. These results provide us with an understanding of variations in dust events in East Asia from changes in climate.

Accelerated Arctic warming over the past decades has led to a large retreat of Arctic sea ice (Comiso 2002; Boé et al. 2009; Overland and Wang 2010; Cohen et al. 2014). The changes in surface albedo associated with melting snow and ice will exacerbate warming in the Arctic (Holland and Bitz 2003; Serreze and Francis 2006), especially in winter (Screen and Simmonds 2010a; Serreze and Barry 2011; Kim and Kim 2018; Dai et al. 2019). Winter Arctic warming has been enhanced by increasing oceanic heat loss, which is likely the combination of the direct response to reductions in the fall/winter ice cover, and the indirect response to summer sea ice loss and increased summer ocean heating (Screen and Simmonds 2010b). In addition, other mechanisms also partially contribute to the accelerated warming of the Arctic, including local forcing and feedbacks (Goosse et al. 2018; Stuecker et al. 2018), increased water vapor and clouds (Bintanja et al. 2011; Taylor et al. 2013; Pithan and Mauritsen 2014; Burt et al. 2016), increased poleward energy transport (Cai 2005; Gong et al. 2017), and the other thermodynamic processes (Chylek et al. 2009; Yoo et al. 2011; Screen et al. 2012; Ding et al. 2014; Franzke et al. 2016; Screen and Francis 2016; Yoshimori et al. 2017). Observations indicated that diminishing sea ice is the major driver of Arctic amplification (Serreze et al. 2009; Screen and Simmonds 2010a; Crook et al. 2011; Taylor et al. 2013; Yim et al. 2016). The Arctic amplification caused by the increase in outgoing longwave radiation and heat flux in the new open sea occurs only over areas where sea ice is significantly reduced, thus the sea ice retreat is necessary for large amplification happening in the Arctic (Dai et al. 2019). Here, "Arctic amplification" refers to surface warming over the Arctic, which has been nearly twice as large as warming over the rest of the globe in recent decades (Rigor et al. 2000; Polyakov et al. 2002; Serreze and Francis 2006; Graversen et al. 2008; Serreze et al. 2009; Screen and Simmonds 2010a, b). The loss of Arctic ice cover may affect large-scale atmospheric circulation

patterns (Jaiser et al. 2013; Pedersen et al. 2016), and thus influence northern mid- and high-latitude climate (Deser et al. 2007, 2010; Petoukhov and Semenov 2010; Liu et al. 2012; Li and Wang 2013, 2014; Mori et al. 2014). Therefore, there is an urgent need to explore the impact of winter Arctic amplification on the remarkable decline in spring dust event occurrences over northern China.

Until now, meteorological parameters and climate teleconnections have been used individually to investigate long-term variations in dust event occurrences. However, thermodynamic processes related to the connection of spring dust event occurrences with winter Arctic amplification still need to be performed. The remainder of this paper is organized as follows. Section 2 presents the data and methods used in the research. In Sect. 3, firstly the Arctic amplification is described in detail, then we use the Empirical orthogonal function (EOF) analysis to investigate the temporal and spatial variations of spring dust index over northern China (70° E–140° E, 30° N–55° N). Then, atmospheric circulations and climate conditions connected winter Arctic amplification with decline in spring dust events over northern China for 1961–2014 are presented. Finally, we explore that the change in dust event occurrences over northern China related to Arctic amplification in the future by using the Fifth Climate Models Intercomparison Project (CMIP5) models. The conclusion and discussion is presented in Sect. 4. We believe that results presented here provide a comprehensive and detailed analysis of the thermodynamic processes involved in reduction of spring dust events over northern China with winter Arctic amplification, and help advance in climate models on dust aerosol. It should be noted that winter (December–January–February) appearing in the following study is in the winter of 1960–2013, and spring is in the spring (March–April–May) of 1961–2014.

2 Data and methods

2.1 Datasets

Datasets of daily dust event occurrences (dust storm, blowing dust, and floating dust) during the period of 1961–2014 are derived from surface meteorological observations over mainland China. The Dust (storm) Subject Databases (V1.0) is provided by the National Meteorological Center of China. The three types of dust events have been identified by several previous studies (Wang et al. 2005, 2008, 2018a; Kang et al. 2016). Briefly, the dust storm is defined as large quantities of dust particles transported in the atmosphere (Visibility < 1 km), whereas floating dust is defined as suspended dust derived from upwind sources (Visibility < 10 km) on a given day. The definition of blowing dust is similar to that of floating dust, but for dust that is emitted from local sources. Dust events frequently occur in spring over northern China (Zhou and Zhang 2003), related to strong winds, thermal instability, and dust sources. The Dust (storm) Subject Databases contains information for more than 2400 sites (basic, benchmark weather stations and general weather stations) in China. The datasets of dust event occurrences, visibility, daily maximum wind speed, and wind direction contain observations from ground stations beginning in January 1954. The climatic threshold value or allowable value check, internal consistency check, and spatial consistency check are applied to control the weather phenomena and visibility data. The valid data of every element is > 98%, and the correct rate of the dataset is close to 100%, so the dataset is considered to be of high quality. Additionally, to minimize the uncertainties of data, apart from the quality control of the dataset itself, a series of stringent quality controls is in place before using the product. (1) If missing days in record at a site are greater than 10 days in a certain month, this month is omitted. (2) If missing months in record at a site are equal or greater than one month in a certain year, this year is omitted. (3) After the step (1) and (2), sites with the annual statistics for less than 40 of years during 1961–2014 are excluded. We have reduced a handful of poor-quality sites based on the above quality control steps, and 1506 stations are remained in the 1613 stations within the latitude more than 30° N over northern China finally.

A dataset of sea ice concentration for 1979–2014 from the National Aeronautics and Space Administration (NASA) Scanning Multichannel Microwave Radiometer (SMMR) and the Special Sensor Microwave/Imager (SMM/I) (Cavalieri et al. 1999), which is obtained from the National Snow and Ice Data Center (NSIDC; http://nsidc.org/data) is used in this work. Sea-ice extent (SIE) is defined as the total area with at least 15% sea-ice concentration. The Arctic SIE index is calculated as the area-averaged SIE in the region north of 70° N in fall (September–October–November). The snow cover data used in this paper is obtained from the Rutgers University Global Snow Lab (Robinson et al. 1993), and can be downloaded freely from https://climate.rutgers.edu/snowcover/docs.php?target=datareq. The original data are mapped on the 89 × 89 cell Northern Hemisphere grids from October 1966 to the present, with cell resolution ranging from 10,700 to 41,800 km^2, which is interpolated to a 2.5° × 2.5° resolution here.

The GISS surface temperature analysis (GISTEMP) dataset is an estimate of global surface temperature change with a resolution of 2° × 2° from the NASA Goddard Institute for Space Studies (GISS) from 1880 to the present day (Hansen et al. 2010), and is available at https://data.giss.nasa.gov/gistemp/. The precipitation dataset used in this study is the Global Precipitation Climatology Center (GPCC) monthly precipitation dataset (Schneider et al. 2018), with a spatial resolution of 2.5° × 2.5°, from 1891 to 2016, and is available

at https://opendata.dwd.de/climate_environment/GPCC/html/fulldata-monthly_v2018_doi_download.html. The soil moisture data is from the Climate Prediction Center (CPC) of the National Oceanic and Atmospheric Administration, at a 0.5°×0.5° resolution from 1948 to the present (Dool et al. 2003; Mitchell and Jones 2005). The data is available at https://www.esrl.noaa.gov/psd/data/gridded/data.cpcsoil.html. It is interpolated to a 2.5°×2.5° resolution for our study.

The reanalysis data employed in this study are from the National Centers for Environmental Prediction-National Center for Atmospheric Research (NCEP/NCAR), which is achieved by combining a fixed global data assimilation system and model, along with a comprehensive database of land surface, radiosonde, pibal, ship, aircraft, satellite, and other data. It includes analyses of the atmosphere at 17 pressure levels at a resolution of 2.5°×2.5° from 1948 to the present, and is available at https://www.esrl.noaa.gov/psd/data/gridded/data.ncep.reanalysis.html (Kalnay et al. 1996; Kistler et al. 2001). We use the monthly mean fields of wind, sea level pressure (SLP) and geopotential height in the winter and spring during the period of 1961–2014.

The historical simulations during 1961–2005 and future predictions for Representative Concentration Pathways (RCPs) RCP4.5 and RCP8.5 during 2006–2099 are obtained from the Fifth Climate Models Intercomparison Project (CMIP5) used in this study. The datasets of dust emission flux, temperature, precipitation, snow cover, and soil moisture content were statistically simulated by 49 models from the CMIP5, which are interpolated to 1°×1° spatial resolution. Moreover, we only selected the first ensemble run from all these models (Taylor et al. 2012). There are only 14 out of 49 models simulate dust emission flux, while only 5 models simulate all climatic factors related to Asian dust occurrences in this study. However, we found that the discrepancy due to inconsistent multi-model ensemble for different climatic factors can be neglected for the projections. Pierce et al. (2009) exhibited that the ensemble mean of model simulation is superior to individual model. Therefore, we prefer to analyze the results based on the ensemble mean of the relevant models for each climatic factor in this study. The relative models used in this study are shown in Table 1, and are available at https://cera-www.dkrz.de/WDCC/ui/cerasearch/q?query=cmip5&page=0&rows=15.

2.2 Calculation of dust index

Previous studies have explored dust events and have found significant differences in their relative concentrations (Qian et al. 2002; Shao and Wang 2003; Zhu et al. 2008). Niu et al. (2001) found that the mass concentration of the dust-storm category is almost three times greater than that of blowing dust, and nine times greater than that of floating dust. Therefore, Wang et al. (2008) developed a new dust index based on the daily frequency of dust storm, blowing dust, and floating dust at four observational stations near dust sources (e.g. Gobi Desert and Taklimakan Desert). The dust index can better characterize the regional statistically and large-scale nature of dust events. In this study, the dust index is estimated using the following equation described by Wang et al. (2008):

$$\text{Dust index} = \text{FD} \times 1 + \text{BD} \times 3 + \text{DS} \times 9, \tag{1}$$

where FD, BD, and DS represent the total days of floating dust, blowing dust and dust storm on a given month at a site, respectively. It is worth noting that the value of 1 represents the normalized mass weight of dust aerosols for each floating dust episode, while three and nine represent the relative mass weight of dust aerosols for blowing dust and dust storm, respectively. Based on the above equation, we can estimate the spring dust index by calculating the regional average of dust index for 1506 sites over northern China from March to May for 1961–2014. The dust index used in this study can represent the intensities of all kinds of dust events over northern China. The combination of regional stations used here effectively represents the large-scale nature of the dust events.

2.3 Calculation of the surface temperature gradient

To understand large-scale atmospheric circulation dynamics caused by the winter Arctic amplification and their impact on climate in mid-latitude areas, we calculate the temperature gradient using the method defined by Soon and Legates (2013), who modified the method used by Jain et al. (1999) and Karamperidou et al. (2012) for gradients that exist in the meridional direction only, so the areal weighting is removed in the method. The temperature gradient is calculated as:

$$\text{Temperature gradient} = \frac{\sum_{i=1}^{n}(T_i - \bar{T})\left(\theta_i - \bar{\theta}\right)}{\sum_{i=1}^{n}(\theta_i - \bar{\theta})^2}, \tag{2}$$

where θ_i is the latitude and T_i is the temperature of the ith zonally averaged grid box (n total boxes) and the overbar indicates a hemispheric/latitudinal band average. Each latitudinal band is averaged in the zonal direction and the temperature gradient is equivalent to the unweighted regression slope of these zonal averages. The gradient used in this study is calculated from 0°N to 80° N within the longitude range 30° E–120° E based on the GISTEMP monthly average data in winter and spring for 1961–2014, in units of °C per latitude. The temperature gradient indices calculated from the GISTEMP data here are anomalies from the average temperature gradient. Because the polar temperature is typically lower than that at the equator, the average temperature gradients are strongly negative generally. Hence,

Table 1 List of CMIP5 used in this study with brief descriptions

		Mrsos			Emidust			Pr			Snc			Tas		
		Historical	RCP4.5	RCP8.5	Historical	RCP4.5	RCP8.5	Historical	RCP4.5	RCP8.5	Historical	RCP4.5	RCP8.5	Historical	RCP4.5	RCP8.5
1	ACCESS1-0		1	1	1	1	1	1	1	1				1	1	1
2	ACCESS1-3		1	1				1	1	1				1	1	1
3	bcc-csm1-1	1	1	1				1	1	1	1	1	1	1	1	1
4	bcc-csm1-1-m	1	1	1				1	1	1	1	1	1	1	1	1
5	BNU-ESM	1	1	1				1	1	1	1	1	1	1	1	1
6	CanCM4	1	1					1	1							
7	CanESM2*	1	1	1	1	1	1	1	1	1	1	1	1	1	1	1
8	CCSM4	1	1	1							1	1	1	1	1	1
9	CESM1-BGC	1	1	1							1	1	1	1	1	1
10	CESM1-CAM5	1	1	1						1	1	1	1	1	1	1
11	CESM1-CAM5-1-FV2		1	1					1							
12	CESM1-FASTCHEM	1									1			1		
13	CESM1-WACCM	1									1			1		
14	CM5A-MR		1													
15	CMCC-CESM							1		1						
16	CMCC-CM								1	1						
17	CMCC-CMS							1	1	1						
18	CNRM-CM5	1		1				1	1	1	1	1	1	1	1	1
19	CNRM-CM5-2	1						1			1			1		
20	CSIRO-Mk3-6-0		1	1	1	1	1	1	1	1	1	1	1	1	1	1
21	FGOALS-g2		1	1				1	1	1	1	1	1	1	1	1
22	FIO-ESM							1	1	1	1	1	1	1	1	1
23	GFDL-CM2p1							1	1					1		
24	GFDL-CM3	1	1	1	1	1	1	1	1	1				1	1	1
25	GFDL-ESM2G	1	1	1				1	1	1				1	1	1
26	GFDL-ESM2M	1	1	1				1	1	1				1	1	1
27	GISS-E2-H		1	1				1	1	1	1	1	1	1	1	1
28	GISS-E2-H-CC	1	1	1				1	1	1	1	1		1	1	1
29	GISS-E2-R	1	1	1				1	1	1	1	1	1	1	1	1
30	GISS-E2-R-CC	1	1	1				1	1	1	1	1		1	1	1
31	HadCM3	1	1					1	1					1		
32	HadGEM2-AO							1	1	1				1		
33	HadGEM2-CC	1	1	1	1	1	1	1	1	1						
34	HadGEM2-ES	1	1	1	1	1	1	1	1	1						

Table 1 (continued)

		Mrsos			Emidust			Pr			Snc			Tas		
		Historical	RCP4.5	RCP8.5	Historical	RCP4.5	RCP8.5	Historical	RCP4.5	RCP8.5	Historical	RCP4.5	RCP8.5	Historical	RCP4.5	RCP8.5
35	inmcm4		1	1				1	1	1	1	1	1	1	1	1
36	IPSL-CM5A-LR	1	1	1				1	1	1				1	1	1
37	IPSL-CM5A-MR	1		1				1	1	1				1	1	1
38	IPSL-CM5B-LR	1	1	1				1	1	1				1	1	1
39	MIROC4h	1	1		1	1		1	1		1	1				
40	MIROC5*	1	1	1	1	1	1	1	1	1	1	1	1	1	1	1
41	MIROC-ESM*	1	1	1	1	1	1	1	1	1	1	1	1	1	1	1
42	MIROC-ESM-CHEM*	1	1	1	1	1	1	1	1	1	1	1	1	1	1	1
43	MPI-ESM-LR							1	1	1	1	1	1	1	1	1
44	MPI-ESM-MR							1	1	1	1	1	1	1	1	1
45	MPI-ESM-P							1			1			1		
46	MRI-CGCM3*	1	1	1	1	1	1	1	1	1	1	1	1	1	1	1
47	MRI-ESM1	1		1	1			1		1	1			1		
48	NorESM1-M	1			1	1	1	1	1	1	1	1	1	1	1	1
49	NorESM1-ME	1			1	1	1	1	1	1	1	1	1	1	1	1

The symbols "1" indicate the historical run (1961–2005) and two future scenario runs (RCP4.5 and RCP8.5; 2006–2099) used in this study. The first ensemble run is only used. "mrsos", "emidust", "pr", "snc" and "tas" is the short name of standard output of soil moisture content, dust emission flux, precipitation, snow cover and surface air temperature respectively. The 5 models marked with "*" simulate all climatic factors related to dust occurrences

positive temperature gradient anomalies in this study represent a weakened temperature gradient, whereas negative values indicate an enhanced temperature gradient.

2.4 Calculation of the NAM index

To further analyze the impact of Arctic climate on dust event occurrences over northern China, we also provide the Northern Hemisphere annular mode (NAM), which represents the "seesaw" phenomenon of air quality between mid-latitude and high-latitude. The NAM is the dominant atmospheric variability in the extratropical regions of Northern Hemisphere (Limpasuvan and Hartmann 2000; Kerr 2001). It can affect the near-surface climate in the mid-high latitudes including China and even in some tropical regions (Kerr 1999; Gong et al. 2001; Thompson and Wallace 2001; Li et al. 2008; Wu et al. 2009). Therefore, the variation in NAM is perhaps one of the major linkages between climate change over Arctic and reduce in dust event occurrences over northern China.

In this study, the NAM index is calculated as the difference in the normalized monthly zonal-mean SLP 35° N and 65° N, which was firstly defined by Li and Wang (2003):

$$I_{NAM} = P_{35°N} - P_{65°N}, \quad (3)$$

the index is obviously superior to that based on the empirical orthogonal function firstly proposed by Thompson and Wallace (1998) in characterizing the spatial pattern of NAM (Angell 2006; Gao et al. 2010). Furthermore, the variations in NAM in Northern Hemisphere were widely performed to investigate the recent climate by previous studies (Angell 2006; Merzlyakov et al. 2009; Gao et al. 2010; Wu et al. 2012).

3 Results

3.1 Arctic amplification

Arctic amplification is a distinguishing feature of warming over the period 1961–2014 in the GISTEMP dataset (Fig. 1). The maximum Arctic warming is found north of 70° N (Fig. 1a), with a more distinct warming trend (up to 0.7 °C/decade) north of 60° N in winter (Fig. 1b), as noted by Huang et al. (2016). It has been suggested that the Arctic region underwent strong warming because of changes in cloud cover (Schweiger et al. 2008), increase in atmospheric water vapor (Francis and Hunter 2007), increased atmospheric heat transport from lower latitudes (Graversen et al. 2008) and declining sea ice (Serreze et al. 2007; Stroeve et al. 2007; Comiso et al. 2008; Screen and Simmonds 2010a). Previous studies have indicated that diminishing sea

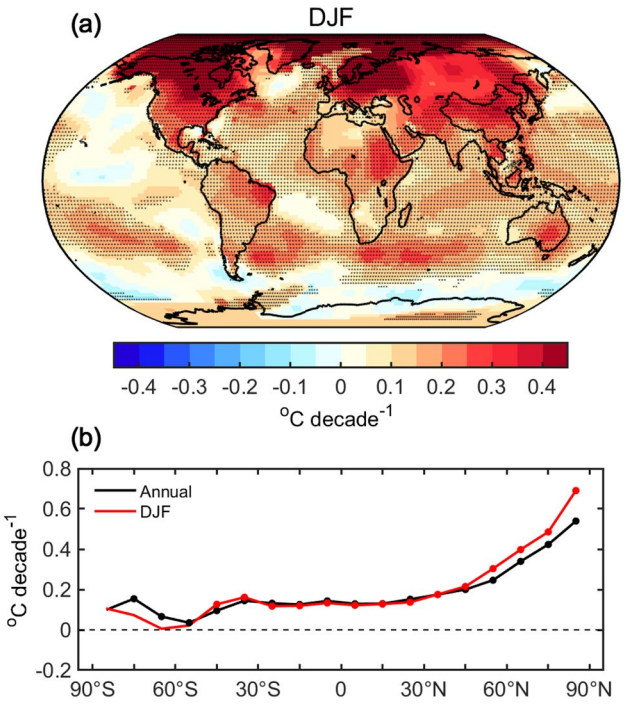

Fig. 1 **a** Linear trend of annual surface air temperature (units: °C decade^{-1}) during 1961–2014. The dotted regions represent correlations required for significance at the 95% level. **b** The zonally averaged linear trends (units: °C decade^{-1}) of annual (black) and winter (DJF, December–January–February; red) mean surface air temperatures from 1961–2014. The dots represent correlations required for significance at the 95% level

ice has played a leading role in recent Arctic temperature amplification (Screen and Simmonds 2010a; Dai et al. 2019), by contributing to an increase in Arctic SST through positive feedback processes related to the decrease of Arctic sea ice (Screen and Simmonds 2010a, b, 2013; Screen et al. 2013). Figure 2a shows the areas covered with sea ice concentrations accounting for 80% in fall season during the period of 1979–2014. Arctic sea ice decreased dramatically over this period in the Barents and Kara Seas, northern Europe, and the Bering Sea in the North Pacific, which is consistent with numerous past studies (Petoukhov and Semenov 2010; Inoue et al. 2012; Jaiser et al. 2012; Cohen et al. 2014). Since the 1980s, Arctic SIE decreased rapidly, at a rate of -5.1×10^4 km^2 per year in the fall during 1979–2014. In addition, a better correlation between the fall SIE and winter surface air temperature is found in the Arctic (70° N–90° N; R of −0.72), compared with that in the region (0° N–70° N; R of −0.47) (Fig. 2b).

3.2 Spatiotemporal variations in dust index

Long-term variations in dust event occurrences in East Asia have been investigated by many previous studies (Fan and

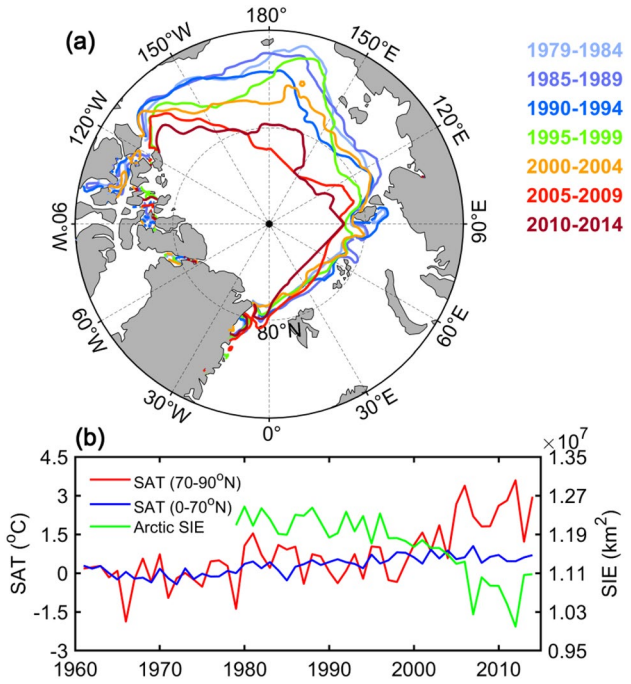

Fig. 2 **a** Distribution of areas with sea ice concentrations accounting for 80% in the fall (SON, September–October–November) for the period 1979–2014. **b** Time series of fall sea-ice extent (SIE; green) over Arctic for 1979–2014, and winter (DJF) surface air temperature (SAT) anomaly relative to the 1961–1990 annual mean in Arctic (north of 70° N; red) and in the latitude range 0° N–70° N (blue) for 1961–2014. The correlation coefficient between sea ice and surface air temperature in Arctic (in the latitude range of 0° N–70° N) is −0.72 (−0.47) for 1979–2014, statistically significant above the 99% confidence level

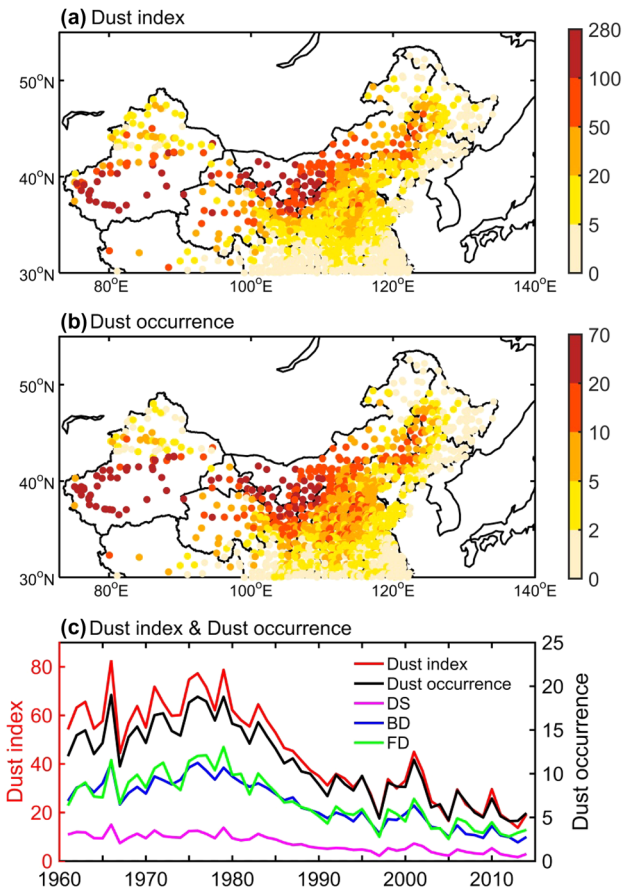

Fig. 3 **a** The climatology of spring (MAM, March–April–May) dust index at 1506 stations over northern China during 1961−2014. **b** Same as **a** but for spring dust occurrence (units: day) at 1506 stations. **c** Time series of spring dust index (red), dust occurrence (black), dust storm occurrence (DS; purple), blowing dust occurrence (BD; blue) and floating dust occurrence (FD; green) in northern China from 1961 to 2014

Wang 2004; Ding et al. 2005; Gong et al. 2006a). However, these studies mainly concentrate on the long-term variations of dust storm associated with relative climatic factors before 2005, which potentially ignored the climate effects of blowing dust and floating dust (Zhao et al. 2004; Gong et al. 2006a; Mao et al. 2011a, b). As illustrated by Wang et al. (2018a), dust events—not only dust storm, but also floating dust and blowing dust—have decreased dramatically since the beginning of this century. However, how winter Arctic amplification in influencing spring dust activities remains unknown. To investigate the thermodynamic processes of the dust events reduction over northern China, a dust index combining dust storm, blowing dust and floating dust over northern China is developed in this study, which also been performed by previous studies (Wang et al. 2008; Kang et al. 2016). The climatology in spring dust index (Fig. 3a) shows a similar pattern to that in spring dust occurrence (Fig. 3b) at 1506 stations. In addition, the temporal variability shows a striking decrease between dust index and dust occurrence compared with three types of dust events (dust storm, floating dust and blowing dust) over northern China since 1980s (Fig. 3c), which is consistent with the previous study by Wang et al. (2018a). It indicated that the dust index is an advanced indicator to present the spatial–temporal evolution and long-term variability of dust events, which is also applied in Tibet Plateau by Kang et al. (2016).

Figure 4 shows the spatiotemporal patterns of dust index anomalies in spring during the period of 1961–2014 over northern China by applying EOF analysis. The EOF analysis can reveal anomaly patterns averaged over the entire period of the study. The first EOF mode (EOF1) accounts for 56.2% of the variability of dust index, and reflects uniform reduction over northern China. Significant decreases are found in the Xinjiang's Taklamakan Desert and the Inner Mongolian's Gobi Desert (Fig. 4a). This pattern is consistent with that of Wang et al. (2018a), who found reductions in dust storm, blowing dust, and floating dust of 76.7%, 68.5%, and 64.5%, respectively, in 2000–2014 compared with the period of 1960–1999 over China. The normalized first principal component (PC1)

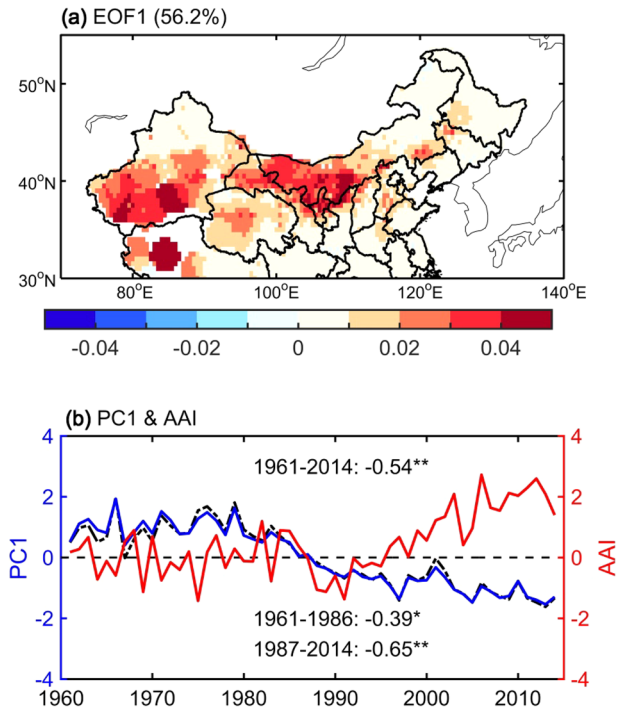

Fig. 4 **a** The spatial pattern of the first leading EOF of spring dust index anomalies for 1961–2014. **b** The time series of normalized first principal component (PC1; blue), spring dust index (black dotted line) over northern China and winter Arctic amplification index (AAI; red; units: °C) for 1961–2014. The * and ** represent correlation required for significance at the 95% and 99% level, respectively

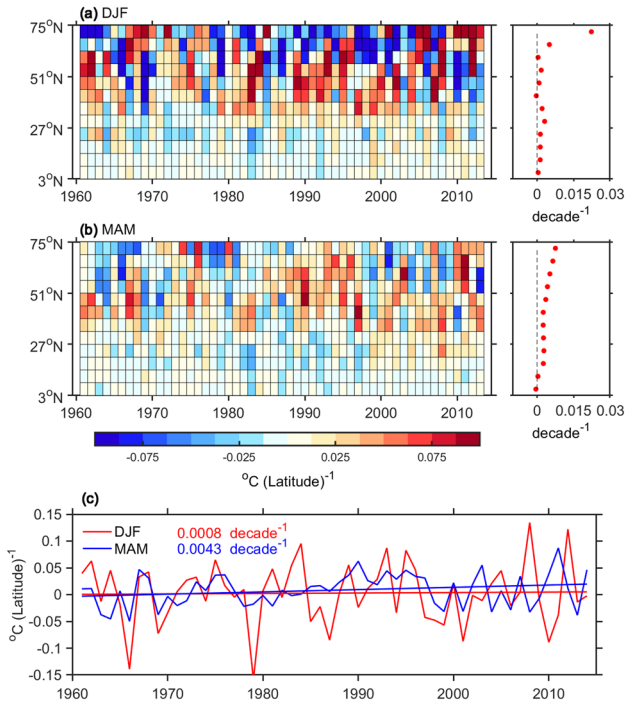

Fig. 5 **a**, **b** The left column is the evolution of the temperature gradient anomalies (units: °C (latitude)$^{-1}$) at bins of 6 latitudes from 0 to 80° N within the longitude range 30° E–120° E in winter (DJF) and spring (MAM) for 1961–2014, respectively. The right column is the linear trends of temperature gradient anomalies during 1961–2014 for the corresponding latitude band. **c** The time series of surface temperature gradient anomalies between 40° N and 70° N in winter (DJF; red) and spring (MAM; blue)

is basically consistent with the normalized original dust index, and describes a negative linear trend with a distinct decline beginning in the 1980s (Fig. 4b). Moreover, an Arctic Amplification index (AAI) is defined in this study to measure the intensity of Arctic amplification. The AAI is the difference between mean surface air temperature (SAT) anomaly in Arctic (north of 70° N) and mean SAT anomaly in the globe. It found that the PC1 of spring dust index and winter AAI exhibit a strong negative correlation. The correlation is − 0.54 during the period of 1961–2014, exceeding the 99% significant level, but the linear correlation for 1961–1986 (− 0.39, only exceeding the 95% significant level) is lower than that during the period of 1987–2014 (− 0.65, exceeding the 99% significant level). These results show that the enhanced Arctic amplification in winter caused by global warming is likely to be one of the dominant factors to influence dust events reduction in spring over northern China since the mid-1980s. Previous study showed that the warming around Lake Baikal has reduced the occurrences of spring dust storm over northern China (Zhu et al. 2008). However, the winter Arctic amplification in affecting spring dust events over northern China under global warming is unknown. The detailed mechanisms still need to be explored.

3.3 Thermodynamic processes

To further investigate the relationship between Arctic amplification and spring dust index over northern China, the spatiotemporal evolution of the temperature gradient in winter and spring for 1961–2014 is shown in Fig. 5. Positive temperature gradient anomalies occur in the areas of 30° N–60° N, with maximum values above 0.075 °C/latitude in winter (Fig. 5a). In spring, temperature gradient anomalies exist basically positive in the middle latitudes of Northern Hemisphere since the mid-1980s (Fig. 5b), which indicates that the temperature gradient is weakened (warmer pole and colder equator). Moreover, temperature gradient anomalies undergo consistently increasing trend between 40° N and 70° N in winter and spring, that is, the temperature gradient is weakened (Fig. 5c). In Northern Hemisphere, the interaction of the rapidly warming Artic and sea ice retreat along with other polar thermodynamic processes makes the warming of Artic areas more remarkable under conditions of global warming (Yoo et al. 2011; Taylor et al. 2013; Ding et al. 2014; Yoshimori et al. 2017; Goosse et al. 2018; Dai et al. 2019). The magnitude of temperature gradient anomalies is larger in winter than those in spring due to the enhanced

Arctic amplification in winter. However, the linear trends of temperature gradient anomalies in spring between 40° N and 70° N are much larger than that in winter during the period of 1961–2014 (Fig. 5a, b). That indicates that the temperature gradient becomes weakened more significantly in spring over Northern Hemisphere, thereafter, leads to a significant decline of westerly wind in the mid-high latitudes as a whole (Deser et al. 2015; Screen et al. 2018; Vavrus 2018; Li et al. 2019).

To investigate the relations between the atmospheric circulation associated with winter Arctic amplification and spring dust events since the 1960s, we perform the linear regression analysis using the wind fields at 200 hPa and 850 hPa in winter and spring on normalized AAI during the period of 1961–2014, respectively (Fig. 6). According to the enhanced Arctic amplification, the wind speed in winter is substantially larger in upper layer in middle latitudes (30° N–50° N), while lower in high latitudes (60° N–80° N) (Fig. 6a). Compared with Fig. 6a, there is no remarkable reduction of wind speed between 40° N and 60° N in spring over East Asia (Fig. 6b). Generally speaking, the wind speed on lower-level over the middle-low latitudes becomes obviously weakened in winter and spring under the stronger Arctic amplification, especially over northern China in spring (Fig. 6c, d). As a result, the winter Arctic amplification can obviously impact the surface wind fields in spring in Northern Hemisphere. To further analyze the possible mechanisms of the decreased wind speed, we also demonstrated the latitude-height cross-section linear trends of wind fields within the longitude range of 73° E–120° E during the period of 1961–2014 in Fig. 7. In winter, the subtropical westerly jet strengthens significantly and westerly wind in high latitudes weakens markedly on upper-level (Fig. 7a), and then the changes weaken in the following spring (Fig. 7b). On the contrary, changes in wind are more

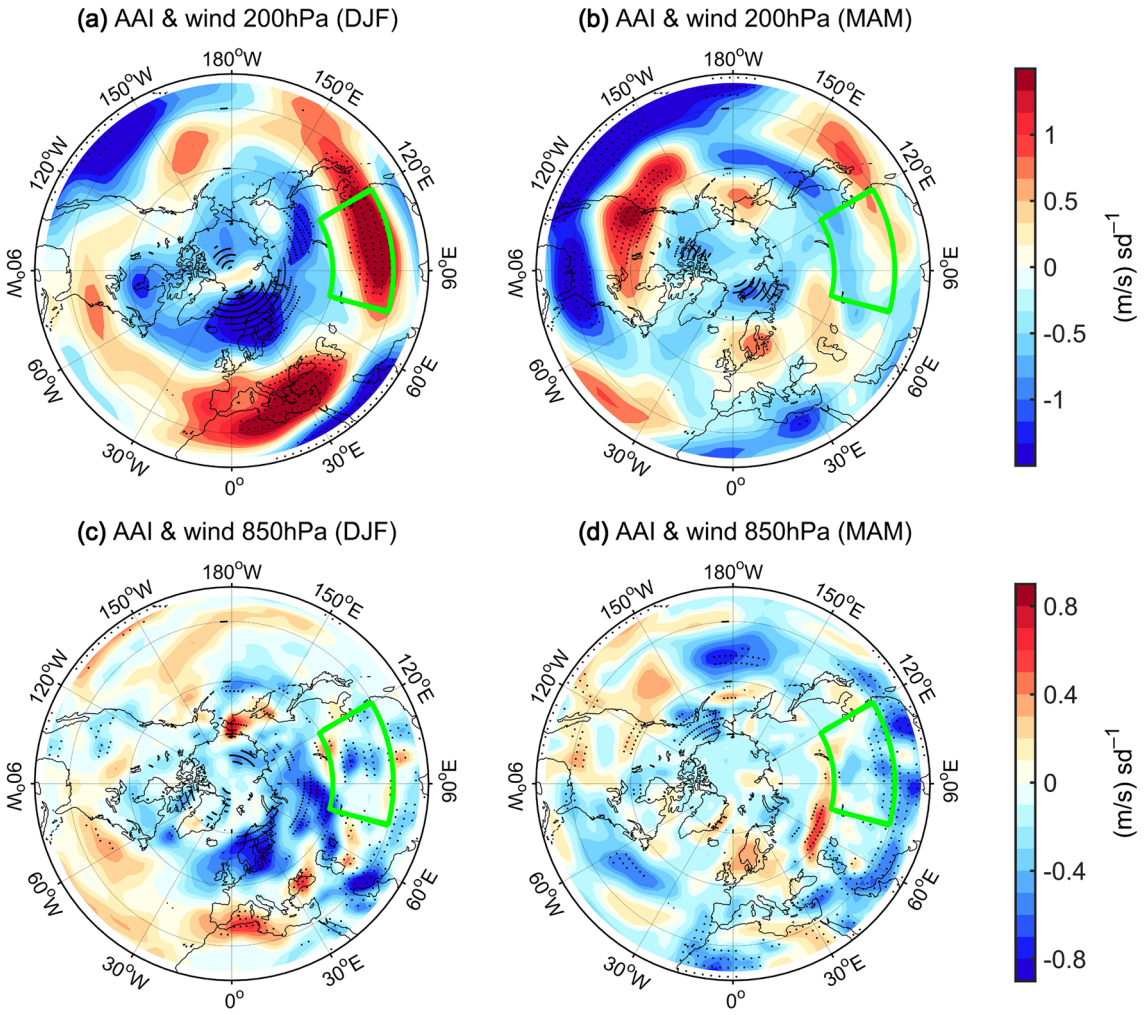

Fig. 6 **a**, **b** Linear regression of 200 hPa wind speed (units: m/s sd^{-1}) in winter (DJF) and spring (MAM) on normalized AAI during 1961–2014, respectively. **c**, **d** Same as **a**, **b** but for 850 hPa wind speed (units: m/s sd^{-1}). The dotted regions represent correlations required for significance at the 95% level. The boxes (75–120° E, 30–50° N) represent the study areas

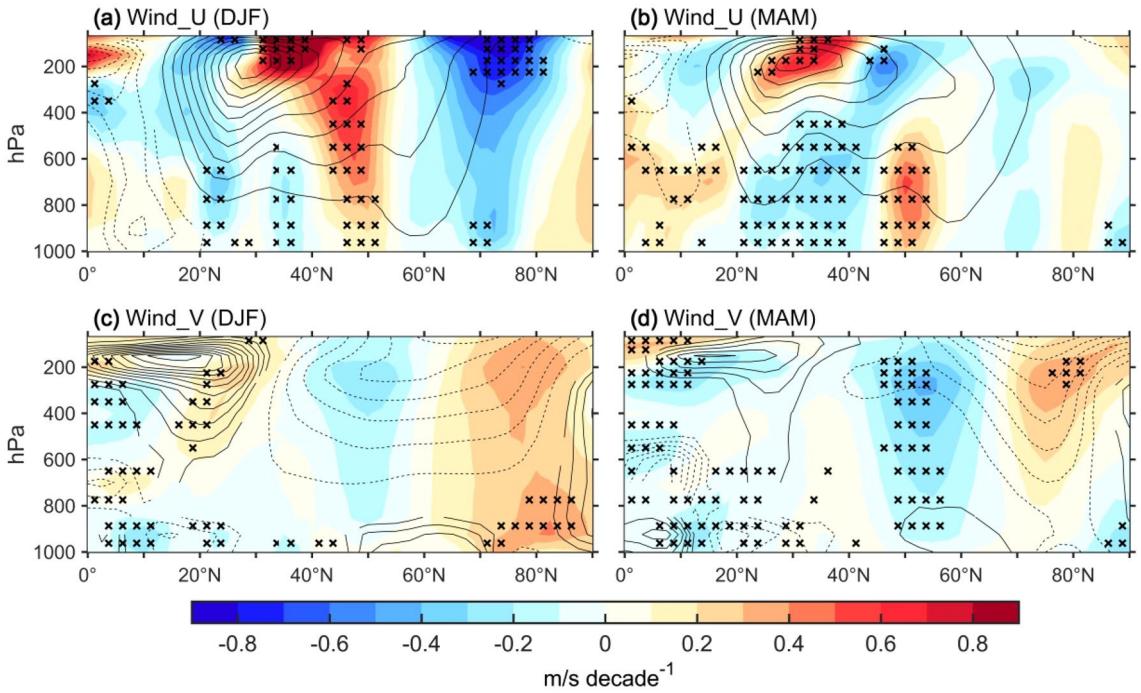

Fig. 7 **a**, **b** Latitude-height cross-section linear trend of zonal wind speed (units: m/s decade^{-1}) in winter (DJF) and spring (MAM) during 1961–2014 respectively, within the longitude range 73° E–120° E. **c**, **d** Same as **a**, **b** but for the meridional wind speed. The black contours indicate the baseline climatology during 1961–2014, the solid line is west wind and the dotted line is east wind in **a**, **b** while the solid line is south wind and the dotted line is north wind in **c**, **d**. The crossed regions represent correlations required for significance at the 95% level

obvious on lower-level in spring. The significant reduction of westerly wind is located over the mid-latitude (20° N–45° N) below 400 hPa (Fig. 7b), and the north wind weakens in the whole layer between 50° N and 60° N in spring (Fig. 7d). The changes of wind in the lower troposphere indicate a northward route of cold air and correspond to the reduction of cold front activities over East Asia. Therefore, the atmospheric circulation changes provide dynamical conditions which are conducive to reducing occurrences of dust event in spring over northern China, as described by Wang et al. (2018a).

To investigate the impacts of the stronger Arctic amplification in winter on the rapid reduction in dust occurrences in spring over northern China since the mid-1980s, we analyzed the changes in wind and geopotential height fields around 1987. The composite fields of 200 hPa and 850 hPa wind in winter and spring separately, for 1987–2014 minus those in 1961–1986 are shown in Fig. 8. Results illustrate that westerly wind enhances significantly in mid-latitude at 200 hPa (Fig. 8a), which is consistent with that in Fig. 7a. The south wind anomaly is shown in the mid-high latitudes, indicating the north wind becomes weakened, especially in spring (Fig. 8b, d). Compared with the wind anomaly for 850 hPa in winter (Fig. 8c), there is a stronger divergent wind in Mongolia and a weaker convergence wind over the East European Plain on lower level (850 hPa) in spring (Fig. 8d).

Moreover, we also show the composite fileds of SLP and 500 hPa geopotential height in winter and spring separately, for 1987–2014 minus those in 1961–1986 (Fig. 9). The lower SLP is substantially associated with an anomalous cyclonic circulation over Europe, while higher SLP is related to an anomalous anticyclonic circulation over Mongolia and northern China after 1980s (Fig. 9a, b). Thence, sea ice reduces in the Barents Sea by warm moisture is transported from north Atlantic and Norwegian Sea to the Barents Sea and Europe due to the anomalous cyclonic circulation, then enhancing the Arctic amplification phenomenon (Fan et al. 2017). Moreover, the 500 hPa geopotential height anticyclonic anomaly over the Mongolian Plateau and central Siberia, and the cyclonic anomaly over the East European Plain and Scandinavian Peninsula in winter (Fig. 9c), persist and appear a stronger anticyclonic anomaly in the ensuing spring (Fig. 9d). This is accompanied with the divergent wind in Mongolia and the convergence wind over the East European Plain on lower troposphere in winter and spring (Fig. 8c, d). As a consequence, the 500-hPa geopotential height anticyclonic anomaly over the Mongolian Plateau and central Siberia contribute to the weakened surface northwesterly wind and the increased rainfall in northwest China (Ding et al. 2005; Liu and Ding 2007; Li et al. 2019). These are conducive to the decline of spring dust events over northern China.

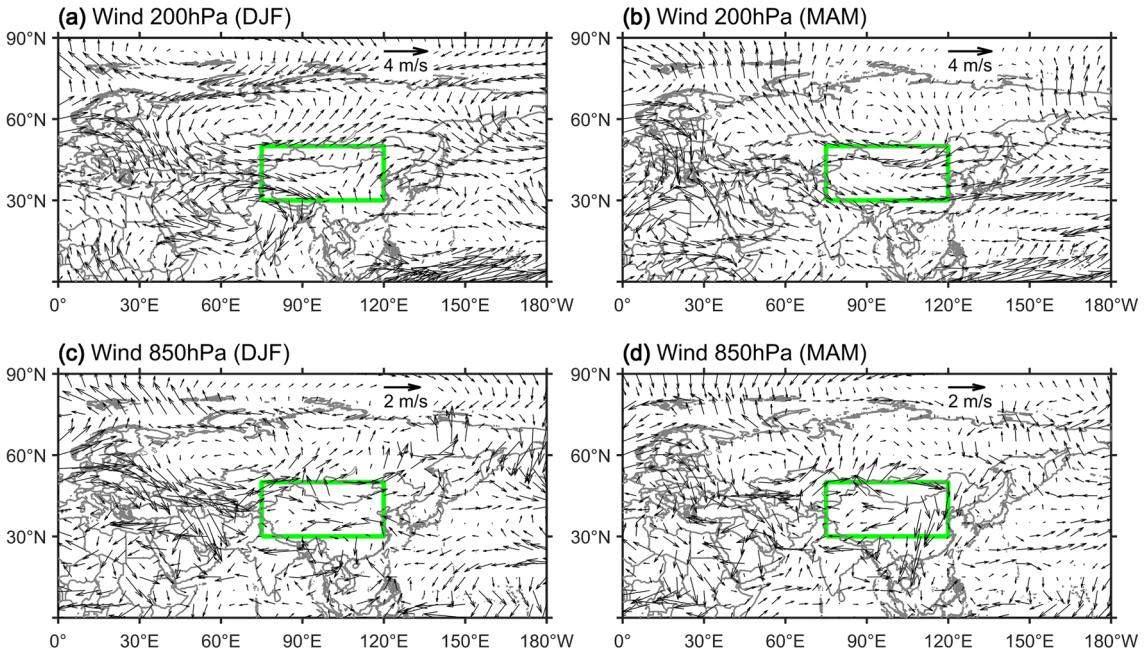

Fig. 8 **a**, **b** Composite analysis of wind (units: m/s) for 200 hPa in winter (DJF) and spring (MAM) during 1987–2014 minus those in 1961–1986, respectively. **c**, **d** Same as **a**, **b** but for 850 hPa. The boxes (75–120° E, 30–50° N) represent the study areas

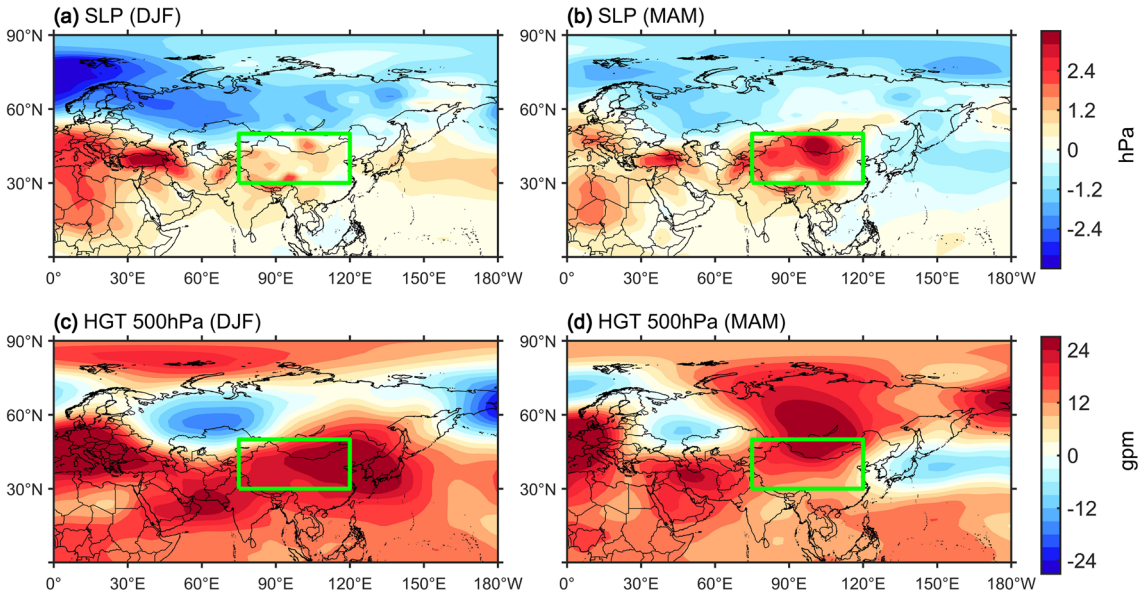

Fig. 9 **a**, **b** Composite analysis of sea level pressure (SLP; units: hPa) in winter (DJF) and spring (MAM) during 1987–2014 minus those in 1961–1986, respectively. **c**, **d** Same as **a**, **b** but for 500 hPa geopotential height (HGT; units: gpm). The boxes (75–120°E, 30–50°N) represent the study areas

We perform the linear regression analysis using the SLP and 500 hPa geopotential height on normalized NAM index in winter and spring during the period of 1961–2014, respectively (Fig. 10). The zonally symmetric pattern associated with a lower SLP in high latitudes and a higher SLP in middle latitudes is remarkable in winter and spring over the Northern Hemisphere, which indicates that the NAM has been enhanced (Fig. 10a, b). The result indicates that a positive phase of NAM is found in the late twentieth century, which is consistent with the previous studies (Miller et al. 2006; Allen and Zender 2011; Mao et al. 2011a, b). Moreover, the NAM in winter is stronger than that in spring.

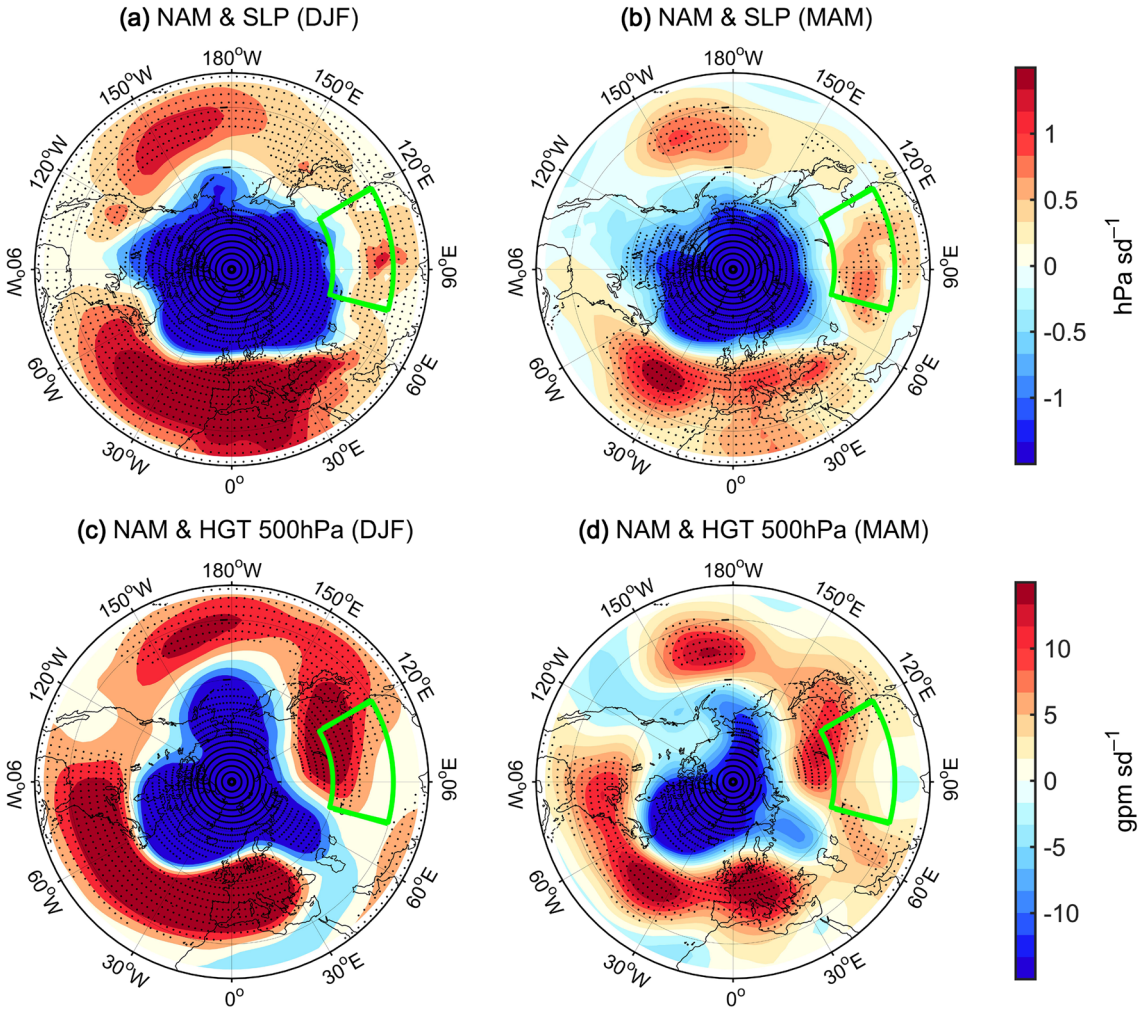

Fig. 10 **a**, **b** Linear regression of SLP (units: hPa sd^{-1}) on normalized northern Hemisphere annular mode (NAM) in winter (DJF) and spring (MAM) during 1961–2014, respectively. **c**, **d** Same as **a**, **b** but for 500 hPa HGT (units: gpm sd^{-1}). The dotted regions represent correlations required for significance at the 95% level. The boxes (75–120° E, 30–50° N) represent the study areas

Previous studies pointed out that the winter NAM can impact climate change over the East Asia (Gong et al. 2001; Liu and Ding 2007; Yin et al. 2013; Li et al. 2019). The similar patterns to SLP are also shown in 500 hPa geopotential height fields in winter and spring (Fig. 10c, d). There is a higher geopotential height associated with an anticyclonic anomaly in the Mongolia region, while a lower geopotential height is dominated by a cyclonic anomaly in the East Europe in winter and spring (Fig. 10c, d). These changes can reduce the Mongolian cyclone frequency, and weaken the surface westerly wind over northern China (Ding et al. 2005; Liu and Ding 2007; Mao et al. 2011a, b). Thus, the decline in cold air activity from higher latitudes into the dryland regions of northwestern China causes a decline in convective activity in these areas. This process may result in a reduction of the dust event occurrences in these regions (Taklimakan Desert and Gobi Desert), and thus reduces the transmission of dust aerosol to the upper and middle troposphere due to a weakened westerly wind in upper-level over northern China. As a result, dust events have been reduced throughout northern China since 1980s.

3.4 The role of climatic factors

A below-normal Eurasian snow cover area in winter persists in the ensuing spring, resulting in a 500 hPa geopotential height anticyclonic anomaly over the Mongolia and Siberia and a cyclonic anomaly over the East European Plain in spring (Kang and Wang 2005; Gong et al. 2007), which have an impact on the cold air activities in East Asia and affect the atmospheric circulation related to occurrences of dust event over northern China. In addition, previous studies have shown that warmer surface air temperatures in winter are favorable for less spring dust weather (Zhu et al. 2008;

Ji and Fan 2019). Over northern China, warm anomaly in winter can lead to a thinner frozen soil layer, when a warmer temperature in following spring, resulting in slighter desertification compared with a deeper frozen soil layer caused by cold anomalies, and less sandy soil provides a fewer dust source for dust weather. Additionally, more precipitation and higher soil moisture in spring over northern China also reduces dust sources.

We also perform a linear regression analysis using snow cover, precipitation and soil moisture in winter and spring on negative PC1 of spring dust index during the period of 1961–2014 (Fig. 11). It is worth noting that the decreased dust index is highly consistent with less snow cover over Europe in winter (Fig. 11a) and over Eurasia in spring (Fig. 11b). Meanwhile, the increased precipitation and soil moisture are beneficial to reduce dust emissions over northern China in winter and spring (Fig. 11c, f). The similar patterns with Fig. 11 are shown in Fig. 12, which present the linear regression of these climatic factors on AAI. Therefore, the stronger Arctic amplification in winter can decrease snow cover over Eurasia, significantly increase precipitation and soil moisture over Asia in spring (Fig. 12). In brief, less spring snow cover in Eurasia acts as a bridge in the relationship between Arctic amplification in winter and dust events in spring over northern China, and affects regional and remote atmospheric circulation in spring through the snow albedo and hydrology effects (e.g., Barenett et al. 1989; Wu and Kirtman 2007; Zuo et al. 2012; Yin et al. 2013). Moreover, anomalies in precipitation and soil moisture in spring related to decreased dust index are similar to those identified in winter. Spring vegetation cover also increases across northern China (not shown) due to increased precipitation and greater soil moisture, and this is agreed with result of Zou and Zhai (2004). Therefore, the aforementioned changes in climate conditions from winter and spring are favorable for decreasing dust events over northern China.

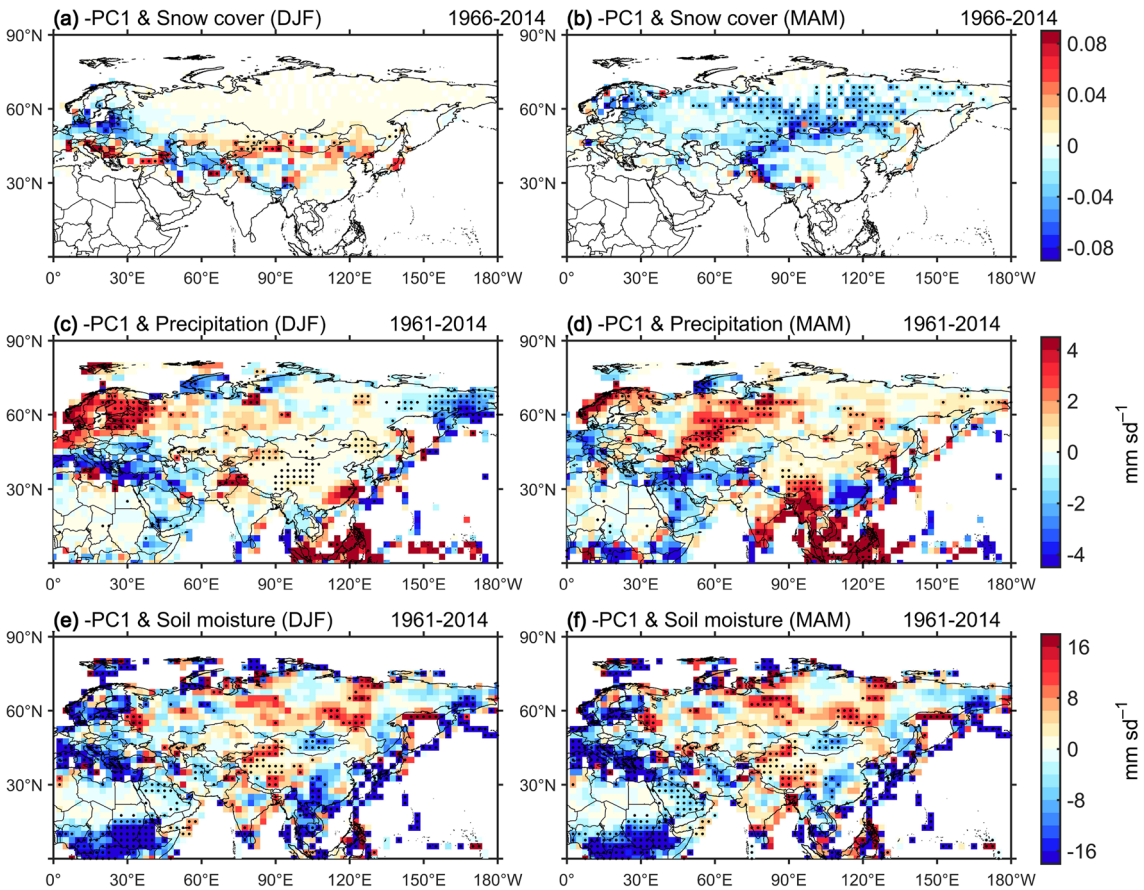

Fig. 11 **a**, **b** Linear regression of snow cover (units: sd^{-1}) in winter (DJF) and spring (MAM), on negative PC1 of spring dust index during 1966–2014, respectively. **c**, **d** Same as **a**, **b** but for precipitation during 1961–2014 (units: mm sd^{-1}). **e**, **f** Same as **a**, **b** but for soil moisture during 1961–2014 (units: mm sd^{-1}). The dotted regions represent correlations required for significance at the 95% level

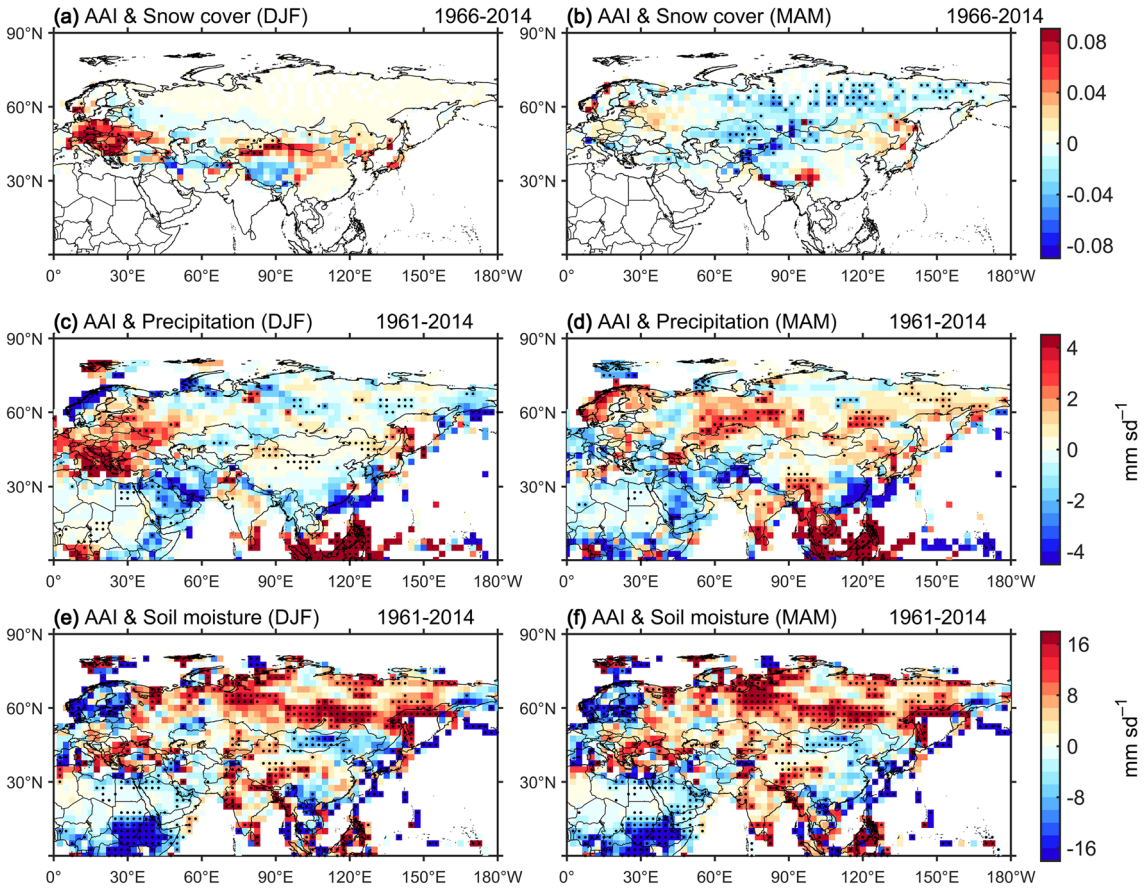

Fig. 12 Same as Fig. 11, but linear regression on normalized AAI

3.5 Future projection of dust aerosol emission

To further capture the reasonable linkage between Arctic amplification and dust event occurrences over northern China, we also investigate the predictions of the future dust emission over northern China during the period of 2006–2099 based on 49 coupled models obtained from the Coupled Model Intercomparison Project phase 5 (CMIP5). Figure 13 shows the time series of surface air temperature over Northern Hemisphere, snow cover over Eurasia (0–180° E, north of 30° N), as well as dust emission flux, precipitation and soil moisture content over northern China (75–115° E, 35–50° N) for a midrange mitigation emissions scenario (RCP4.5) and a high emissions scenario (RCP8.5) during 2006–2099 relative to 2006–2025 in winter and spring, respectively. Results indicated that the winter temperature increases much higher than that in spring, especially for RCP8.5 experiment. The increasing trend is up to 0.55 °C/decade, which exceeds the 99% significant level (Fig. 13a, b). In the future projection, the dust emission over northern China decreases significantly, which is consistent with the increased temperature over Northern Hemisphere (Fig. 13c, d), with the decreased trend of − 0.1 (g/m^2)/decade in spring for RCP8.5, exceeding the 99% significant level. Additionally, the snow cover extent remarkably reduces in Eurasia in winter and continues into early spring, with the comparative trends of − 0.004 per decade for RCP4.5 and − 0.01 per decade for RCP8.5 (Fig. 13e, f). The increased precipitation in spring is more significant than that in winter over northern China, with a maximum value of 3.13 mm/decade for RCP8.5, exceeding the 99% significant level (Fig. 13g, h). The soil moisture content over northern China is significantly increased in winter and spring for RCP4.5, while a slight decrease for RCP8.5 in spring (Fig. 13i, j). We found that soil moisture content increases over northwest China for RCP8.5 more obviously than that for RCP4.5, which also agree well with the previous study by Cheng et al. (2017). Therefore, the increased precipitation and soil moisture over northern China both contribute to the increase of local vegetation. As a result, the soil became wetter for a warm climate, thereafter, disturb to produce less dust emissions.

Finally, the spatial variations of observed dust index, as well as simulated dust emission flux in spring for history and future projection are given in Fig. 14. Compared with observed dust index in Fig. 14a, the models can simulate well the long-term trends of dust emissions from CMIP5

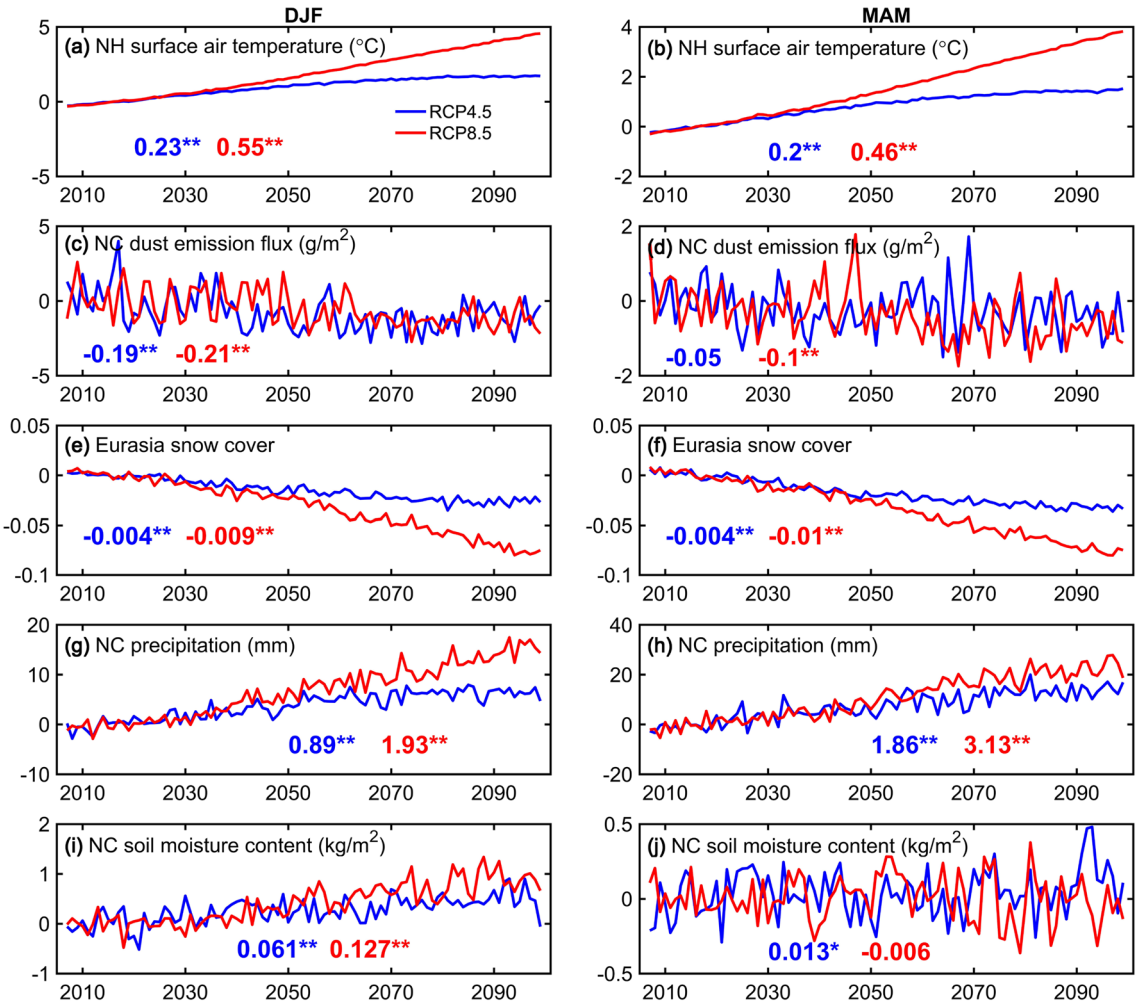

Fig. 13 **a**, **b** The time series of surface air temperature (units: °C) over Northern Hemisphere (NH) for CMIP5 RCP4.5 (blue) and RCP8.5 (red) in winter (DJF) and spring (MAM) during 2006–2099 relative to 2006–2025, respectively. **c**, **d** Same as **a**, **b** but for dust emission flux (units: g/m^2) over northern China (NC; 75–115° E, 35–50° N). **e**, **f** Same as **a**, **b** but for snow cover over Eurasia (0–180° E, north of 30° N). **g**, **h** Same as **a**, **b** but for precipitation (units: mm) over northern China. **i**, **j** Same as **a**, **b** but for soil moisture content (units: kg/m^2) over northern China. Values shown in figures are linear trends (units:/decade) from 2006 to 2099, and the * and ** represent correlation required for significance at the 95% and 99% level, respectively

historical experiment during 1987–2005 minus those in 1961–1986, especially in the Taklimakan and Gobi Deserts over northern China (Fig. 14b). The result is also similar with the previous study by Wu et al. (2018a). As shown in Fig. 14c, the dust emissions in spring can decrease up to − 8 g/m^2 in Gobi Desert regions for 2071–2090 relative to 2006–2025 for RCP4.5 in the future projection. The spring dust emissions decrease remarkably by the late 21th century. The maximum decline of dust emission is up to − 4 g/m^2 and − 8 g/m^2 in Taklimakan and Gobi Desert regions during the period of 2071–2090 relative to 2006–2025 for RCP8.5, respectively (Fig. 14d).

To estimate the sensitivity due to multi-model ensemble, we compared the linear trends of ensemble means of the relevant models for each climatic factor and that of the selected 5 models simulated all climatic factors for historical experiments during 1961–2005 and future projections during 2006–2099 (Fig. 15). We found that the trends are consistent for different multi-model ensemble means in winter and spring, especially for future projections (RCP4.5 and RCP8.5). Additionally, the trends of different multi-model ensemble means are comparative for dust emission flux and the relevant climatic factors in spring. It indicated that the discrepancy due to inconsistent multi-model ensemble for different climatic factors can be neglected for the projections. As a summary, we found that the above climate parameters change more significantly for RCP8.5 than that for RCP4.5, especially for temperature, snow cover and precipitation. The reduction of dust emission in spring for RCP8.5 is larger than that for RCP4.5 in the future as global

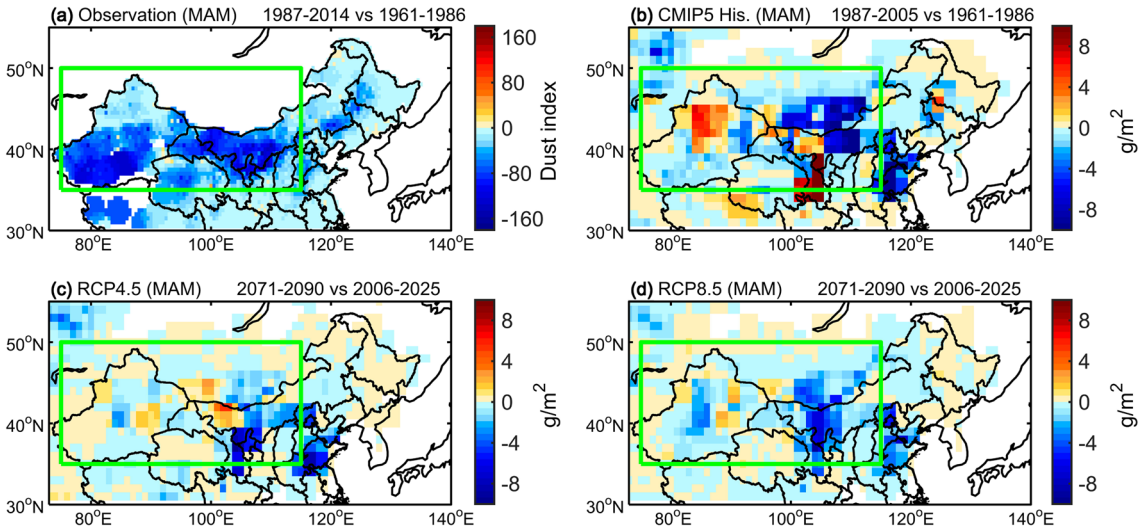

Fig. 14 **a** Composite analysis of dust index in spring (MAM) during 1987–2014 minus those in 1961–1986 based on observation data. **b** Same as **a** but for dust emission flux (units: g/m^2) from CMIP5 historical experiment during 1987–2005 minus those in 1961–1986. **c** Same as **b** but for CMIP5 RCP4.5 experiment during 2071–2090 minus those in 2006–2025. **d** Same as **b** but for CMIP5 RCP8.5 experiment during 2071–2090 minus those in 2006–2025. The boxes represent the areas: Northern China (75–115° E, 35–50° N)

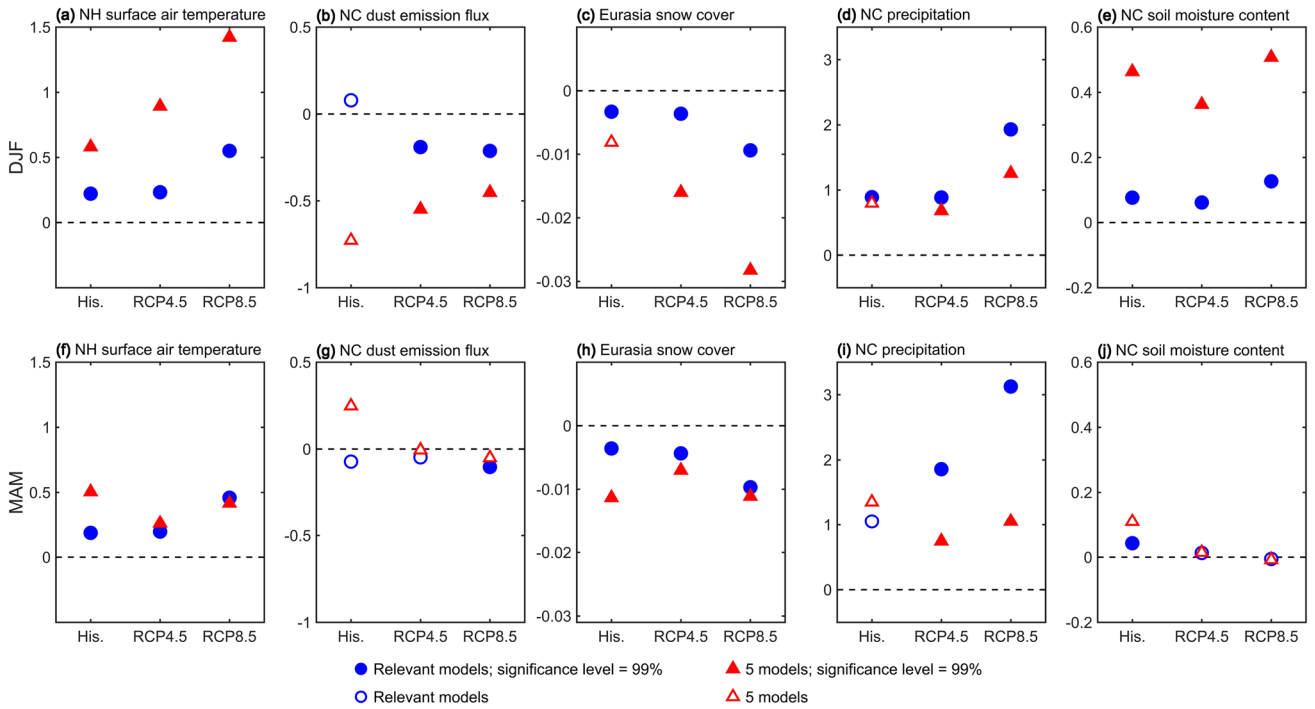

Fig. 15 **a**, **f** The linear trends of surface air temperature (units: °C/decade) over Northern Hemisphere (NH) for CMIP5 models for historical experiments (His.) during the period of 1961–2005 and for the future projection (RCP4.5 and RCP8.5) during the period of 2006–2099, in winter (DJF) and spring (MAM) respectively. **b**, **g** Same as **a**, **f** but for dust emission flux (units: g/m^2/decade) over northern China (NC; 75–115° E, 35–50° N). **c**, **h** Same as **a**, **f** but for snow cover (units:/decade) over Eurasia (0–180° E, north of 30° N). **d**, **i** Same as **a**, **f** but for precipitation (units: mm/decade) over northern China. **e**, **j** Same as **a**, **f** but for soil moisture content (units: kg/m^2/decade) over northern China. The circles and triangles represent the linear trends of ensemble means for the relevant CMIP5 models and the selected 5 CMIP5 models respectively, and the solid circles and triangles represent correlation required for significance at the 99% level

temperatures continue to rise. These results indicated that the Arctic amplification could lead a key role in leading the decline of dust event occurrences over northern China.

4 Conclusion and discussion

In recent years, changes in weather events in the mid-high latitudes of the Northern Hemisphere related to Arctic amplification have been receiving ever-increasing attention worldwide (Francis and Vavrus 2012; Barnes 2013; Screen and Simmonds 2013; Cohen et al. 2014). Dust events in spring are regarded among the most severe disasters over northern China, and their influence in East Asia grows with the population and economy (Wang et al. 2004). However, the relationship between long-term variability in dust event occurrences in spring over northern China and Arctic amplification in winter has not been directly investigated in detail.

The purpose of this study is to explore the impact of Arctic amplification in winter related to the retreat of Arctic sea ice on the occurrences of dust event in spring over northern China in a warming world. We first calculated a dust index that accounts for dust storm, blowing dust and floating dust over northern China (north of 30° N) based on the definition of Wang et al. (2008). The first leading pattern of dust index anomaly over northern China in spring for 1961–2014 was obtained by applying the leading empirical orthogonal function (EOF) analysis, accounting for 56.2% of variability in dust index. Here, we showed that the decline of spring dust events over northern China has a strong relationship with winter Arctic amplification because of global warming since the 1980s. As a result of Arctic amplification, dust event occurrences have been significantly reduced over northern China since the mid-1980s due to weakened meridional temperature gradients and zonal winds over Northern Hemisphere. Moreover, positive sea level pressure anomalies associated with the anticyclonic activity in spring over East Asia during the positive NAM phase can reduce the cold air activities in mid-latitude (Wu and Kirtman 2007). The spring dust emission over northern China may continue decreasing under the global warming in the future.

The thermodynamic mechanisms between the decline of dust events over northern China and Arctic amplification are summarized in Fig. 16. It is worth noting that the enhanced Arctic amplification and stronger NAM in winter, through decline of snow cover in Eurasia, induces the anticyclonic anomalies over Siberia and Mongolia and cyclonic anomalies over East Europe in spring (Yang et al. 2002). The decreased westly wind is dominated by the weakened temperature gradients in the mid-latitude (Yin et al. 2013; Wang et al. 2018a; Li et al. 2019). More precipitation and higher soil moisture in spring over northern China have an obvious influence on the atmospheric circulation (Gong et al. 2007; Kang and Wang 2005; Wu and Wang 2002). Finally, the decline of cold air activities in East Asia and weakened westly winds in the mid-latitude may contribute to the reduction of dust event occurrences in spring over northern China since 1980s.

Although we now have an improved understanding of the mechanisms of dust events reduction in spring over northern China associated with winter Arctic amplification, many potential factors contributing to dust event occurrences remain to be explored. Land cover changes, the impact of human activities, and other climate teleconnections may partly be responsible for the secular decrease in dust event

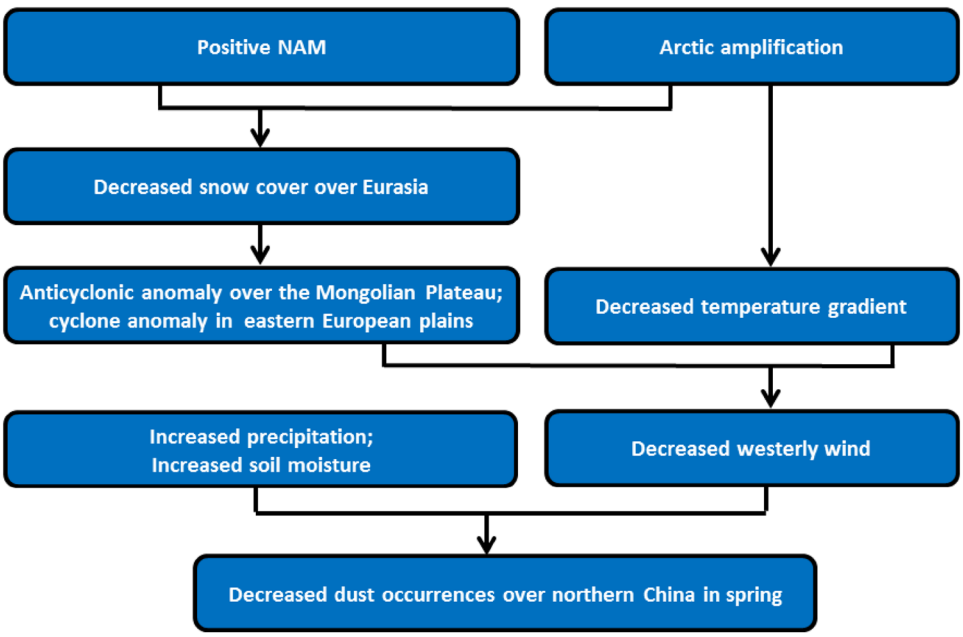

Fig. 16 Decline of dust events in northern China linking Arctic amplification and associated impacts related to climate indices

occurrences over northern China. Thus, future research should be done to investigate mechanisms of dust reduction related to these factors, and clarify their relative contributions to the decline of dust events over northern China. Furthermore, researches have shown that spring dust activities are closely related to El Niño-Southern Oscillation (ENSO), mainly via the variations in dust transport paths rather than those in dust occurrences in dust source areas (e.g. Hara et al. 2006; Lee et al. 2014). The Pacific decadal oscillation (PDO) is linked to variations and deposition of dust aerosols not only in the eastern North Pacific and North America but also in spring dust source regions over East Asia, with fewer dust aerosols during the warm phase of the PDO (Gong et al. 2006b). Thus, mechanisms connected the interdecadal variability of dust events over northern China with the variability of the SST patterns associated with global warming, as ENSO, PDO and Atlantic Multidecadal Oscillation (AMO), are expected to be further explored to clarify their relative contributions.

Acknowledgements This research was supported jointly by the National Key R&D Program of China (2019YFA0606801), the National Natural Science Foundation of China (Grants 41775144, 41571039, 41675065, and 41875091), and the Fundamental Research Funds for the Central Universities (lzujbky-2018-k02).

References

Ackerman AS, Toon OB, Stevens DE, Heymsfield AJ, Ramanathan V, Welton EJ (2000) Reduction of tropical cloudiness by soot. Science 288:1042–1047. https://doi.org/10.1126/science.288.5468.1042

Allen RJ, Zender CS (2011) Forcing of the arctic oscillation by eurasian snow cover. J Clim. https://doi.org/10.1175/2011JCLI4157.1

Andreae MO, Rosenfeld D (2008) Aerosol–cloud–precipitation interactions. Part 1. The nature and sources of cloud-active aerosols. Earth Sci Rev 89:13–41. https://doi.org/10.1016/j.earscirev.2008.03.001

Angell JK (2006) Changes in the 300-mb north circumpolar vortex, 1963–2001. J Clim 19:2984–2994. https://doi.org/10.1175/JCLI3778.1

Barenett TP, Dumenil L, Schlese U, Roekler E, Latif M (1989) The effect of Eurasian snow cover on regional and global climate variation. J Atmos Sci 46:661–686. https://doi.org/10.1175/1520-0469(1989)046%3c0661:TEOESC%3e2.0.CO;2

Barnes EA (2013) Revisiting the evidence linking arctic amplification to extreme weather in midlatitudes. Geophys Res Lett 40:4734–4739. https://doi.org/10.1002/grl.50880

Bintanja R, Graversen RG, Hazeleger W (2011) Arctic winter warming amplified by the thermal inversions and consequent low infrared cooling to space. Nat Geosci 4:758–761. https://doi.org/10.1038/ngeo1285

Boé J, Hall A, Qu X (2009) September sea-ice cover in the Arctic Ocean projected to vanish by 2100. Nat Geosci 2:341–343. https://doi.org/10.1038/ngeo467

Burt MA, Randall DA, Branson MD (2016) Dark warming. J Clim 29:705–719. https://doi.org/10.1175/JCLI-D-15-0147.1

Cai M (2005) Dynamical amplification of polar warming. Geophys Res Lett 32:L22710. https://doi.org/10.1029/2005GL024481

Cavalieri DJ, Parkinson CL, Gloersen P, Comiso JC, Zwally HJ (1999) Deriving long-term time series of sea ice cover from satellite passive-microwave multisensor data sets. J Geophys Res Oceans 104:15803–15814. https://doi.org/10.1029/1999jc900081

Che H, Zhang XY, Xia X, Goloub P, Holben B, Zhao H, Wang Y, Zhang XC, Wang H, Blarel L, Damiri B, Zhang R, Deng X, Ma Y, Wang T, Geng F, Qi B, Zhu J, Yu J, Chen Q, Shi G (2015) Ground-based aerosol climatology of china: aerosol optical depths from the china aerosol remote sensing network (CARSNET) 2002–2013. Atmos Chem Phys 15:7619–7652. https://doi.org/10.5194/acp-15-7619-2015

Che H, Xia X, Zhao H, Dubovik O, Holben BN, Goloub P, Cuevas-Agulló E, Estelles V, Wang Y, Zhu J, Qi B, Gong W, Yang H, Zhang R, Yang L, Chen J, Wang H, Zheng Y, Gui K, Zhang X, Zhang X (2019) Spatial distribution of aerosol microphysical and optical properties and direct radiative effect from the China Aerosol Remote Sensing Network. Atmos Chem Phys 19:11843–11864. https://doi.org/10.5194/acp-19-11843-2019

Chen Q, Wang M, Sun H, Wang X, Wang Y, Li Y, Zhang L, Mu Z (2018) Enhanced health risks from exposure to environmentally persistent free radicals and the oxidative stress of PM2.5 from Asian dust storms in Erenhot, Zhangbei and Jinan, China. Environ Int 121:260–268. https://doi.org/10.1016/j.envint.2018.09.012

Cheng S, Huang J, Ji F, Lin L (2017) Uncertainties of soil moisture in historical simulations and future projections. J Geophys Res Atmos 122:2239–2253. https://doi.org/10.1002/2016JD025871

Chiapello I, Moulin C, Prospero JM (2005) Understanding the long term variability of African dust transport across the Atlantic as recorded in both Barbados surface concentrations and large scale Total Ozone Mapping Spectrometer (TOMS) optical thickness. J Geophys Res Atmos. https://doi.org/10.1029/2004JD005132

Chylek P, Folland CK, Lesins G, Dubey MK, Wang MY (2009) Arctic air temperature change amplification and the Atlantic multidecadal oscillation. Geophys Res Lett 36:L14801. https://doi.org/10.1029/2009GL038777

Cohen J, Screen JA, Furtado JC, Barlow M, Whittleston D, Coumou D, Francis J, Dethloff K, Entekhabi D, Overland J, Jones J (2014) Recent Arctic amplification and extreme mid-latitude weather. Nat Geosci 7:627–637. https://doi.org/10.1038/ngeo2234

Comiso JC (2002) A rapidly declining perennial sea ice cover in the Arctic. Geophys Res Lett 29:1956. https://doi.org/10.1029/2002gl015650

Comiso JC, Parkinson CL, Gersten R, Stock L (2008) Accelerated decline in the Arctic sea ice cover. Geophys Res Lett 35:L01703. https://doi.org/10.1029/2007GL031972

Creamean JM, Suski KJ, Rosenfeld D, Cazorla A, DeMott PJ, Sullivan RC, White AB, Ralph FM, Minnis P, Comstock JM, Tomlinson JM, Prather KA (2013) Dust and biological aerosols from the Sahara and Asia influence precipitation in the western U.S. Science 339:1572–1578. https://doi.org/10.1126/science.1227279

Crook JA, Forster PM, Stuber N (2011) Spatial patterns of modeled climate feedback and contributions to temperature response and polar amplification. J Clim 24:3575–3592. https://doi.org/10.1175/2011jcli3863.1

Dai A, Luo D, Song M, Liu J (2019) Arctic amplification is caused by sea-ice loss under increasing CO_2. Nat Commun. https://doi.org/10.1038/s41467-018-07954-9

Deser C, Tomas RA, Peng S (2007) The transient atmospheric circulation response to North Atlantic SST and sea ice anomalies. J Clim 20:4751–4767. https://doi.org/10.1175/jcli4278.1

Deser C, Tomas R, Alexander M, Lawrence D (2010) The seasonal atmospheric response to projected arctic sea ice loss in the late twenty-first century. J Clim 23:333–351. https://doi.org/10.1175/2009jcli3053.1

Deser C, Tomas RA, Sun L (2015) The role of ocean–atmosphere coupling in the zonal-mean atmospheric response to arctic sea ice loss. J Clim 28:2168–2186. https://doi.org/10.1175/JCLI-D-14-00325.1

Ding R, Li J, Wang S, Ren F (2005) Decadal change of the spring dust storm in northwest China and the associated atmospheric circulation. Geophys Res Lett 32:L02808. https://doi.org/10.1029/2004gl021561

Ding Q, Wallace JM, Battisti DS, Steig EJ, Gallant AJE, Kim HJ, Geng L (2014) Tropical forcing of the recent rapid arctic warming in northeastern Canada and Greenland. Nature 509:209–212. https://doi.org/10.1038/nature13260

Dool HVD, Huang J, Fan Y (2003) Performance and analysis of the constructed analogue method applied to US soil moisture over 1981–2001. J Geophys Res Atmos 108:8617. https://doi.org/10.1029/2002JD003114

Duce RA, Unni CK, Ray BJ, Prospero JM, Merrill JT (1980) Long-range atmospheric transport of soil dust from Asia to the tropical North Pacific: temporal variability. Science 209:1522–1524. https://doi.org/10.1126/science.209.4464.1522

Fan K, Wang H (2004) Antarctic oscillation and the dust weather frequency in North China. Geophys Res Lett 31:L10201. https://doi.org/10.1029/2004gl019465

Fan K, Xie Z, Wang H, Xu Z, Liu J (2017) Frequency of spring dust weather in North China linked to sea ice variability in the Barents Sea. Clim Dyn 51:4439–4450. https://doi.org/10.1007/s00382-016-3515-7

Francis JA, Hunter E (2007) Changes in the fabric of the Arctic's greenhouse blanket. Environ Res Lett 2:045011. https://doi.org/10.1088/1748-9326/2/4/045011

Francis JA, Vavrus SJ (2012) Evidence linking Arctic amplification to extreme weather in mid-latitudes. Geophys Res Lett 39:L06801. https://doi.org/10.1029/2012GL051000

Franzke CLE, Lee S, Feldstein SB (2016) Evaluating Arctic warming mechanisms in CMIP5 models. Clim Dyn 48:3247–3260. https://doi.org/10.1007/s00382-016-3262-9

Fu Q, Thorsen TJ, Su J, Ge JM, Huang JP (2009) Test of mie-based single-scattering properties of non-spherical dust aerosols in radiative flux calculations. J Quant Spectrosc Radiat Transfer 110:1640–1653. https://doi.org/10.1016/j.jqsrt.2009.03.010

Gao H, Washington R (2010) Arctic oscillation and the interannual variability of dust emissions from the Tarim Basin: a TOMS AI based study. Clim Dyn 35:511–522. https://doi.org/10.1007/s00382-009-0687-4

Ginoux P, Prospero JM, Torres O, Chin M (2004) Long-term simulation of global dust distribution with the GOCART model: correlation with North Atlantic Oscillation. Environ Modell Softw 19:113–128. https://doi.org/10.1016/S1364-8152(03)00114-2

Gong DY, Wang SW, Zhu JH (2001) East Asian winter monsoon and Arctic oscillation. Geophys Res Lett 28:2073–2076. https://doi.org/10.1029/2000GL012311

Gong DY, Mao R, Fan YD (2006a) East Asian dust storm and weather disturbance: possible links to the Arctic oscillation. Int J Climatol 26:1379–1396. https://doi.org/10.1002/joc.1324

Gong SL, Zhang XY, Zhao TL, Zhang XB, Barrie LA, McKendry IG, Zhao CS (2006b) A simulated climatology of Asian dust aerosol and its trans-pacific transport. Part II: interannual variability and climate connections. J Clim 19:88–103. https://doi.org/10.1175/JCLI3606.1

Gong DY, Mao R, Shi PJ, Fan YD (2007) Correlation between east Asian dust storm frequency and PNA. Geophys Res Lett 34:L14710. https://doi.org/10.1029/2007GL029944

Gong T, Feldstein S, Lee S (2017) The role of downward infrared radiation in the recent Arctic winter warming trend. J Clim 30:4937–4949. https://doi.org/10.1175/JCLI-D-16-0180.1

Goosse H, Kay JE, Armour KC, Bodas-Salcedo A, Chepfer H, Docquier D, Jonko A, Kushner PJ, Lecomte O, Massonnet F, Park HS, Pithan F, Svensson G, Vancoppenolle M (2018) Quantifying climate feedbacks in polar regions. Nat Commun 9:1919. https://doi.org/10.1038/s41467-018-04173-0

Graversen RG, Mauritsen T, Tjernstrom M, Kallen E, Svensson G (2008) Vertical structure of recent Arctic warming. Nature 451:53–56. https://doi.org/10.1038/nature06502

Guo J, Lou M, Miao Y, Wang Y, Zeng Z, Liu H, He J, Xu H, Wang F, Min M, Zhai P (2017) Trans-Pacific transport of dust aerosol originated from East Asia: insights gained from multiple observations and modeling. Environ Pollut 230:1030–1039. https://doi.org/10.1016/j.envpol.2017.07.062

Hansen J, Ruedy R, Sato M, Lo K (2010) Global surface temperature change. Rev Geophys. https://doi.org/10.1029/2010rg000345

Hara Y, Uno I, Wang Z (2006) Long-term variation of Asian dust and related climate factors. Atmos Environ 40:6730–6740. https://doi.org/10.1016/j.atmosenv.2006.05.080

Holland MM, Bitz CM (2003) Polar amplification of climate change in coupled models. Clim Dyn 21:221–232. https://doi.org/10.1007/s00382-003-0332-6

Hsu SC, Huh CA, Lin CY, Chen WN, Mahowald NM, Liu SC, Chou CCK, Liang MC, Tsai CJ, Lin FJ, Chen JP, Huang YT (2012) Dust transport from non-East Asian sources to the North Pacific. Geophys Res Lett 39:L12804. https://doi.org/10.1029/2012gl051962

Huang J, Lin B, Minnis P, Wang T, Wang X, Hu Y, Yi Y, Ayers JK (2006) Satellite-based assessment of possible dust aerosols semi-direct effect on cloud water path over East Asia. Geophys Res Lett 33:L19802. https://doi.org/10.1029/2006gl026561

Huang J, Liu J, Chen B, Nasiri S (2015) Detection of anthropogenic dust using CALIPSO lidar measurements. Atmos Chem Phys 15:11653–11665. https://doi.org/10.5194/acp-15-11653-2015

Huang J, Xie Y, Guan X, Li D, Ji F (2016) The dynamics of the warming hiatus over the Northern Hemisphere. Clim Dyn 48:429–446. https://doi.org/10.1007/s00382-016-3085-8

Huebert BJ, Bates T, Russell PB, Shi G, Kim YJ, Kawamura K, Carmichael G, Nakajima T (2003) An overview of ACE-Asia: strategies for quantifying the relationships between Asian aerosols and their climatic impacts. J Geophys Res 108:8633. https://doi.org/10.1029/2003jd003550

Husar RB, Prospero JM, Stowe LL (1997) Characterization of tropospheric aerosols over the oceans with the NOAA advanced very high resolution radiometer optical thickness operational product. J Geophys Res Atmos 102:16889–16909. https://doi.org/10.1029/96JD04009

Inoue J, Hori ME, Takaya K (2012) The role of barents sea ice in the wintertime cyclone track and emergence of a warm-Arctic cold-Siberian Anomaly. J Clim 25:2561–2568. https://doi.org/10.1175/jcli-d-11-00449.1

Jain S, Lall U, Mann ME (1999) Seasonality and interannual variations of northern hemisphere temperature: equator-to-pole

gradient and ocean-land contrast. J Clim 12:1086–1100. https://doi.org/10.1175/1520-0442(1999)012%3c1086:saivon%3e2.0.co;2

Jaiser R, Dethloff K, Handorf D, Rinke A, Cohen J (2012) Impact of sea ice cover changes on the Northern Hemisphere atmospheric winter circulation. Tellus A 64:11595. https://doi.org/10.3402/tellusa.v64i0.11595

Jaiser R, Dethloff K, Handorf D (2013) Stratospheric response to Arctic sea ice retreat and associated planetary wave propagation changes. Tellus A 65:19375. https://doi.org/10.3402/tellusa.v65i0.19375

Ji L, Fan K (2019) Climate prediction of dust weather frequency over northern China based on sea-ice cover and vegetation variability. Clim Dyn 53:687–705. https://doi.org/10.1007/s00382-018-04608-w

Jickells TD, An ZS, Andersen KK, Baker AR, Bergametti G, Brooks N, Cao JJ, Boyd PW, Duce RA, Hunter KA, Kawahata H, Kubilay N, laRoche J, Liss PS, Mahowald N, Prospero JM, Ridgwell AJ, Tegen I, Torres R (2005) Global iron connections between desert dust, ocean biogeochemistry, and climate. Science 308:67–71. https://doi.org/10.1126/science.1105959

Jin Q, Wei J, Yang ZL (2014) Positive response of Indian summer rainfall to Middle East dust. Geophys Res Lett 41:4068–4074. https://doi.org/10.1002/2014GL059980

Jin Q, Wei J, Yang ZL, Pu B, Huang J (2015) Consistent response of Indian summer monsoon to Middle East dust in observations and simulations. Atmos Chem Phys 15:9897–9915. https://doi.org/10.5194/acp-15-9897-2015

Kalnay E, Kanamitsu M, Kistler R, Collins W, Deaven D, Gandin L, Iredell M, Saha S, White G, Woollen J, Zhu Y, Chelliah M, Ebisuzaki W, Higgins W, Janowiak J, Ropelewski C, Wang J, Leetmaa A, Reynolds R, Jenne R, Joseph D (1996) The NCEP/NCAR 40-year reanalysis project. Bull Am Meteor Soc 77:437–472. https://doi.org/10.1175/1520-0477(1996)077%3c0437:TNYRP%3e2.0.CO;2

Kang DJ, Wang HJ (2005) Analysis on the decadal scale variation of the dust storm in North China. Sci Chin Ser D 48:2260–2266. https://doi.org/10.1360/03yd0255

Kang L, Huang J, Chen S, Wang X (2016) Long-term trends of dust events over Tibetan Plateau during 1961–2010. Atmos Environ 125:188–198. https://doi.org/10.1016/j.atmosenv.2015.10.085

Karamperidou C, Cioffi F, Lall U (2012) Surface temperature gradients as diagnostic indicators of midlatitude circulation dynamics. J Clim 25:4154–4171. https://doi.org/10.1175/jcli-d-11-00067.1

Kaufman YJ, Tanre D, Boucher O (2002) A satellite view of aerosols in the climate system. Nature 419:215–223. https://doi.org/10.1038/nature01091

Kerr RA (1999) A new force in high-latitude climate. Science 284:241–242. https://doi.org/10.1126/science.284.5412.241

Kerr RA (2001) Getting a handle on the north's "El Niño". Science 294:494–495. https://doi.org/10.1126/science.294.5542.494b

Kim JY, Kim KY (2018) Relative role of horizontal and vertical processes in the physical mechanism of wintertime Arctic amplification. Clim Dyn 52:6097–6107. https://doi.org/10.1007/s00382-018-4499-2

Kistler R, Kalnay E, Collins W, Saha S, White G, Woollen J, Chelliah M, Ebisuzaki W, Kanamitsu M, Kousky V, Dool H, Jenne R, Fiorino M (2001) The NCEP–NCAR reanalysis: monthly means CD-ROM and documentation. Bull Am Meteor Soc 82:247–268. https://doi.org/10.1175/1520-0477(2001)082%3c0247:TNNYRM%3e2.3.CO;2

Kurosaki Y, Mikami M (2003) Recent frequent dust events and their relation to surface wind in East Asia. Geophys Res Lett 30:1736. https://doi.org/10.1029/2003gl017261

Lee YG, Kim J, Ho CH, An SI, Cho HK, Mao R, Tian B, Wu D, Lee JN, Kalashnikova O, Choi Y, Yeh SW (2014) The effects of ENSO under negative AO phase on spring dust activity over northern China: an observational investigation. Int J Climatol 35:935–947. https://doi.org/10.1002/joc.4028

Li JP, Wang JLXL (2003) A modified zonal index and its physical sense. Geophys Res Lett 30:1632. https://doi.org/10.1029/2003gl017441

Li F, Wang H (2013) Autumn sea ice cover, winter northern hemisphere annular mode, and winter precipitation in Eurasia. J Clim 26:3968–3981. https://doi.org/10.1175/jcli-d-12-00380.1

Li F, Wang H (2014) Autumn Eurasian snow depth, autumn Arctic sea ice cover and East Asian winter monsoon. Int J Climatol 34:3616–3625. https://doi.org/10.1002/joc.3936

Li J, Yu R, Zhou T (2008) Teleconnection between NAO and climate downstream of the Tibetan Plateau. J Clim 21:4680–4690. https://doi.org/10.1175/2008JCLI2053.1

Li C, Tsay SC, Fu JS, Dickerson RR, Ji Q, Bell SW, Gao Y, Zhang W, Huang J, Li Z, Chen H (2010) Anthropogenic air pollution observed near dust source regions in northwestern China during springtime 2008. J Geophys Res. https://doi.org/10.1029/2009jd013659

Li JP, Zheng F, Sun C, Feng J, Wang J (2019) Pathways of influence of the Northern Hemisphere mid-high latitudes on East Asian climate: a review. Adv Atmos Sci 36:902–921. https://doi.org/10.1007/s00376-019-8236-5

Limpasuvan V, Hartmann DL (2000) Wave-maintained annular modes of climate variability. J Clim 13:4414–4429. https://doi.org/10.1175/1520-0442(2000)013%3c4414:WMAMOC%3e2.0.CO;2

Liu XH, Ding RQ (2007) The relationship between the Spring Asian Atmospheric circulation and the previous winter Northern Hemisphere annular mode. Theor Appl Climatol 88:71–81. https://doi.org/10.1007/s00704-006-0231-y

Liu J, Curry JA, Wang H, Song M, Horton RM (2012) Impact of declining Arctic sea ice on winter snowfall. Proc Natl Acad Sci USA 109:4074–4079. https://doi.org/10.1073/pnas.1114910109

Ma S, Zhang X, Gao C, Tong DQ, Xiu A, Wu G, Cao X, Huang L, Zhao H, Zhang S, Ibarra-Espinosa S, Wang X, Li X, Dan M (2019) Multimodel simulations of a springtime dust storm over northeastern China: implications of an evaluation of four commonly used air quality models (CMAQ v5.2.1, CAMx v6.50, CHIMERE v2017r4, and WRF-Chem v3.9.1). Geosci Model Dev 12:4603–4625. https://doi.org/10.5194/gmd-12-4603-2019

Mao R, Gong D, Bao J, Fan Y (2011a) Possible influence of Arctic oscillation on dust storm frequency in North China. J Geogr Sci 21:207–218. https://doi.org/10.1007/s11442-011-0839-4

Mao R, Ho CH, Shao Y, Gong DY, Kim J (2011b) Influence of Arctic oscillation on dust activity over northeast Asia. Atmos Environ 45:326–337. https://doi.org/10.1016/j.atmosenv.2010.10.020

Merzlyakov EG, Murphy DJ, Vincent RA, Portnyagin YI (2009) Long-term tendencies in the MLT prevailing winds and tides over Antarctica as observed by radars at Molodezhnaya, Mawson and Davis. J Atmos Sol-Terr Phy 71:21–32. https://doi.org/10.1016/j.jastp.2008.09.024

Miller RL, Schmidt GA, Shindell DT (2006) Forced annular variations in the 20th century intergovernmental panel on climate change fourth assessment report models. J Geophys Res Atmos 111:D18101. https://doi.org/10.1029/2005JD006323

Mitchell TD, Jones PD (2005) An improved method of constructing a database of monthly climate observations and associated high-resolution grids. Int J Climatol 25:693–712. https://doi.org/10.1002/joc.1181

Mori M, Watanabe M, Shiogama H, Inoue J, Kimoto M (2014) Robust Arctic sea-ice influence on the frequent Eurasian cold winters

in past decades. Nat Geosci 7:869–873. https://doi.org/10.1038/ngeo2277
Mukai M, Nakajima T, Takemura T (2004) A study of long-term trends in mineral dust aerosol distributions in Asia using a general circulation model. J Geophys Res 109:D19204. https://doi.org/10.1029/2003JD004270
Niu SJ, Sun JM, Chen Y, Liu HJ (2001) Observation and analysis of mass concentration of dust and sand aerosol in spring in Helanshan area. Plateau Meteor 20:82–87 **(Chinese)**
Overland JE, Wang M (2010) Large-scale atmospheric circulation changes are associated with the recent loss of Arctic sea ice. Tellus A 62:1–9. https://doi.org/10.1111/j.1600-0870.2009.00421.x
Pedersen RA, Cvijanovic I, Langen PL, Vinther BM (2016) The impact of regional arctic sea ice loss on atmospheric circulation and the NAO. J Clim 29:889–902. https://doi.org/10.1175/jcli-d-15-0315.1
Petoukhov V, Semenov VA (2010) A link between reduced Barents-Kara sea ice and cold winter extremes over northern continents. J Geophys Res 115:D21111. https://doi.org/10.1029/2009jd013568
Pierce DW, Barnett TP, Santer BD, Gleckler PJ (2009) Selecting global climate models for regional climate change studies. Proc Natl Acad Sci USA 106:8441–8446. https://doi.org/10.1073/pnas.0900094106
Pithan F, Mauritsen T (2014) Arctic amplification dominated by temperature feedbacks in contemporary climate models. Nat Geosci 7:181–184. https://doi.org/10.1038/NGEO2071
Polyakov IV, Alekseev GV, Bekryaev RV, Bhatt U, Colony RL, Johnson MA, Karklin VP, Makshtas AP, Walsh D, Yulin AV (2002) Observationally based assessment of polar amplification of global warming. Geophys Res Lett 29:1878. https://doi.org/10.1029/2001gl011111
Pu W, Wang X, Zhang X, Ren Y, Shi J, Bi J, Zhang B (2015) Size distribution and optical properties of particulate matter (PM_(10)) and black carbon (BC) during dust storms and local air pollution events across a loess plateau site. Aerosol Air Qual Res 15:2212–2224. https://doi.org/10.4209/aaqr.2015.02.0109
Qian WH, Quan LS, Shi SY (2002) Variations of the dust storm in China and its climatic control. J Clim 15:1216–1229. https://doi.org/10.1175/1520-0442(2002)015%3c1216:VOTDSI%3e2.0.CO;2
Rigor IG, Colony RL, Martin S (2000) Variations in surface air temperature observations in the Arctic, 1979–1997. J Clim 13:896–914. https://doi.org/10.1175/1520-0442(2000)013%3c0896:VISATO%3e2.0.CO;2
Robinson DA, Dewey KF, Heim RR (1993) Global snow cover monitoring—an update. Bull Am Meteorol Soc 74:1689–1696. https://doi.org/10.1175/1520-0477(1993)074%3c1689:GSCMAU%3e2.0.CO;2
Rosenfeld D, Rudich Y, Lahav R (2001) Desert dust suppressing precipitation: a possible desertification feedback loop. Proc Natl Acad Sci USA 98:5975–5980. https://doi.org/10.1073/pnas.101122798
Sassen K, DeMott PJ, Prospero JM, Poellot MR (2003) Saharan dust storms and indirect aerosol effects on clouds: CRYSTAL-FACE results. Geophys Res Lett 30:1633. https://doi.org/10.1029/2003gl017371
Schneider U, Becker A, Finger P, Meyer-Christoffer A, Ziese M (2018) GPCC full data monthly product version 2018 at 0.25°: monthly land-surface precipitation from rain-gauges built on GTS-based and historical data. Res Data Arch. https://doi.org/10.5676/DWD_GPCC/FD_M_V2018_025
Schweiger AJ, Lindsay RW, Vavrus S, Francis JA (2008) Relationships between Arctic sea ice and clouds during autumn. J Clim 21:4799–4810. https://doi.org/10.1175/2008JCLI2156.1
Screen JA, Francis JA (2016) Contribution of sea-ice loss to Arctic amplification is regulated by Pacific ocean decadal variability. Nat Clim Change 6:861–865. https://doi.org/10.1038/nclimate3011
Screen JA, Simmonds I (2010a) The central role of diminishing sea ice in recent Arctic temperature amplification. Nature 464:1334–1337. https://doi.org/10.1038/nature09051
Screen JA, Simmonds I (2010b) Increasing fall-winter energy loss from the Arctic ocean and its role in Arctic temperature amplification. Geophys Res Lett 37:L16707. https://doi.org/10.1029/2010gl044136
Screen JA, Simmonds I (2013) Exploring links between Arctic amplification and mid-latitude weather. Geophys Res Lett 40:959–964. https://doi.org/10.1002/grl.50174
Screen JA, Deser C, Simmonds I (2012) Local and remote controls on observed Arctic warming. Geophys Res Lett 39:10709. https://doi.org/10.1029/2012GL051598
Screen JA, Simmonds I, Deser C, Tomas R (2013) The atmospheric response to three decades of observed Arctic sea ice loss. J Clim 26:1230–1248. https://doi.org/10.1175/jcli-d-12-00063.1
Screen JA, Deser C, Smith DM, Zhang X, Blackport R, Kushner PJ, Oudar T, McCusker KE, Sun L (2018) Consistency and discrepancy in the atmospheric response to Arctic sea-ice loss across climate models. Nat Geosci 11:155–163. https://doi.org/10.1038/s41561-018-0059-y
Serreze MC, Barry RG (2011) Processes and impacts of Arctic amplification: a research synthesis. Global Planet Change 77:85–96. https://doi.org/10.1016/j.gloplacha.2011.03.004
Serreze MC, Francis JA (2006) The arctic amplification debate. Clim Change 76:241–264. https://doi.org/10.1007/s10584-005-9017-y
Serreze MC, Holland MM, Stroeve J (2007) Perspectives on the Arctic's shrinking sea-ice cover. Science 315:1533–1536. https://doi.org/10.1126/science.1139426
Serreze MC, Barrett AP, Stroeve JC, Kindig DN, Holland MM (2009) The emergence of surface-based Arctic amplification. The Cryosphere 3:11–19. https://doi.org/10.5194/tc-3-11-2009
Shao Y, Wang J (2003) A climatology of Northeast Asian dust events. Meteor Z 12:187–196. https://doi.org/10.1127/0941-2948/2003/0012-0187
Sokolik IN, Toon OB (1996) Direct radiative forcing by anthropogenic airborne mineral aerosols. Nature 381:681–683. https://doi.org/10.1038/381681a0
Solmon F, Mallet M, Elguindi N, Giorgi F, Zakey A, Konaré A (2008) Dust aerosol impact on regional precipitation over western Africa, mechanisms and sensitivity to absorption properties. Geophys Res Lett 35:L24705. https://doi.org/10.1029/2008gl035900
Soon W, Legates DR (2013) Solar irradiance modulation of Equator-to-Pole (Arctic) temperature gradients: empirical evidence for climate variation on multi-decadal timescales. J Atmos Sol-Terr Phy 93:45–56. https://doi.org/10.1016/j.jastp.2012.11.015
Stroeve J, Holland MM, Meier W, Scambos T, Serreze M (2007) Arctic sea ice decline: faster than forecast. Geophys Res Lett 34:L09501. https://doi.org/10.1029/2007gl029703
Stuecker MF, Bitz CM, Armour KC, Proistosescu C, Kang SM, Xie SP, Kim D, McGregor S, Zhang W, Zhao S, Cai W (2018) Polar amplification dominated by local forcing and feedbacks. Nat Clim Change 8:1076–1081. https://doi.org/10.1038/s41558-018-0339-y
Taylor KE, Stouffer RJ, Meehl GA (2012) An overview of CMIP5 and the experiment design. Bull Am Meteor Soc 93:485–498. https://doi.org/10.1175/BAMS-D-11-00094.1
Taylor PC, Cai M, Hu A, Meehl J, Zhang GJ (2013) A decomposition of feedback contributions to polar warming amplification. J Clim 26:7023–7043. https://doi.org/10.1175/JCLI-D-12-00696.1

Thompson DWJ, Wallace JM (1998) The Arctic oscillation signature in the wintertime geopotential height and temperature fields. Geophys Res Lett 25:1297–1300. https://doi.org/10.1029/98gl00950

Thompson DWJ, Wallace JM (2001) Regional climate impacts of the northern hemisphere Annular Mode. Science 293:85–89. https://doi.org/10.1126/science.1058958

Twomey SA, Piepgrass M, Wolfe TL (1984) An assessment of the impact of pollution on global cloud albedo. Tellus B 36:356–366. https://doi.org/10.3402/tellusb.v36i5.14916

Vavrus SJ (2018) The influence of arctic amplification on mid-latitude weather and climate. Curr Clim Change Rep 4:238–249. https://doi.org/10.1007/s40641-018-0105-2

Wang X, Dong Z, Zhang J, Liu L (2004) The modern dust storms in China: an overview. J Arid Environ 58:559–574. https://doi.org/10.1016/j.jaridenv.2003.11.009

Wang S, Wang J, Zhou Z, Shang K (2005) Regional characteristics of three kinds of dust storm events in China. Atmos Environ 39:509–520. https://doi.org/10.1016/j.atmosenv.2004.09.033

Wang X, Huang J, Ji M, Higuchi K (2008) Variability of East Asia dust events and their long-term trend. Atmos Environ 42:3156–3165. https://doi.org/10.1016/j.atmosenv.2007.07.046

Wang WC, Huang JP, Minnis P, Hu YX, Li JM, Huang ZW, Ayers JK, Wang TH (2010) Dusty cloud properties and radiative forcing over dust source and downwind regions derived from A-Train data during the Pacific Dust Experiment. J Geophys Res Atmos. https://doi.org/10.1029/2010jd014109

Wang WC, Sheng LF, Jin HC, Han YQ (2015a) Dust aerosol effects on cirrus and altocumulus clouds in Northwest China. J Meteor Res 29:793–805. https://doi.org/10.1007/s13351-015-4116-9

Wang X, Pu W, Shi J, Bi J, Zhou T, Zhang X, Ren Y (2015b) A comparison of the physical and optical properties of anthropogenic air pollutants and mineral dust over northwest china. J Meteor Res 29:180–200. https://doi.org/10.1007/s13351-015-4092-0

Wang X, Liu J, Che H, Ji F, Liu J (2018a) Spatial and temporal evolution of natural and anthropogenic dust events over northern China. Sci Rep 8:2141. https://doi.org/10.1038/s41598-018-20382-5

Wang X, Wen H, Shi J, Bi J, Huang Z, Zhang B, Zhou T, Fu K, Chen Q, Xin J (2018b) Optical and microphysical properties of natural mineral dust and anthropogenic soil dust near dust source regions over northwestern China. Atmos Chem Phys 18:2119–2138. https://doi.org/10.5194/acp-18-2119-2018

Wu RG, Kirtman BP (2007) Observed relationship of spring and summer East Asian rainfall with winter and Spring Eurasian snow. J Clim 20:1285–1304. https://doi.org/10.1175/JCLI4068.1

Wu B, Wang J (2002) Winter Arctic oscillation, Siberian high and East Asian winter monsoon. Geophys Res Lett 29:1897. https://doi.org/10.1029/2002GL015373

Wu Z, Wang B, Li J, Jin F (2009) An empirical seasonal prediction model of the east Asian summer monsoon using ENSO and NAO. J Geophys Res 114:D18120. https://doi.org/10.1029/2009JD011733

Wu Y, Zhang R, Han Z, Zeng Z (2010) Relationship between East Asian Monsoon and dust weather frequency over Beijing. Adv Atmos Sci 27:1389–1398. https://doi.org/10.1007/s00376-010-9181-5

Wu Z, Li J, Jiang Z, He J, Zhu X (2012) Possible effects of the North Atlantic Oscillation on the strengthening relationship between the East Asian summer Monsoon and ENSO. Int J Climatol 32:794–800. https://doi.org/10.1002/joc.2309

Wu C, Lin Z, Liu X, Li Y, Lu Z, Wu M (2018a) Can climate models reproduce the decadal change of dust aerosol in East Asia? Geophys Res Lett. https://doi.org/10.1029/2018GL079376

Wu X, Liu J, Wu Y, Wang X, Yu X, Shi J, Bi J, Huang Z, Zhou T, Zhang R (2018b) Aerosol optical absorption coefficients at a rural site in Northwest China: the great contribution of dust particles. Atmos Environ 189:145–152. https://doi.org/10.1016/j.atmosenv.2018.07.002

Yang S, Lau KM, Kim KM (2002) Variations of the East Asian jet stream and Asian–Pacific–American winter climate anomalies. J Clim 15:306–325. https://doi.org/10.1175/1520-0442(2002)015%3c0306:VOTEAJ%3e2.0.CO;2

Yim BY, Min HS, Kim B-M, Jeong JH, Kug JS (2016) Sensitivity of Arctic warming to sea ice concentration. J Geophys Res Atmos 121:6927–6942. https://doi.org/10.1002/2015JD023953

Yin S, Feng J, Li JP (2013) Influences of the preceding winter Northern Hemisphere annular mode on the spring extreme low temperature events in the north of eastern China. Acta Meteor Sinica 71:96–108. https://doi.org/10.11676/qxxb2013.008 **(Chinese)**

Yoo C, Feldstein S, Lee S (2011) Impact of the Madden–Julian Oscillation trend on the polar amplification of surface air temperature during 1979–2008 boreal winter. Geophys Res Lett 38:L24804. https://doi.org/10.1029/2011GL049881

Yoshimori M, Abe-Ouchi A, Laîné A (2017) The role of atmospheric heat transport and regional feedbacks in the Arctic warming at equilibrium. Clim Dyn 49:3457–3472. https://doi.org/10.1007/s00382-017-3523-2

Zhang XY, Gong SL, Zhao TL, Arimoto R, Wang YQ, Zhou ZJ (2003) Sources of Asian dust and role of climate change versus desertification in Asian dust emission. Geophys Res Lett 30:2272. https://doi.org/10.1029/2003gl018206

Zhao C, Dabu X, Li Y (2004) Relationship between climatic factors and dust storm frequency in Inner Mongolia of China. Geophys Res Lett 31:1103. https://doi.org/10.1029/2003gl018351

Zhou ZJ, Zhang GC (2003) Typical severe dust storms in northern China during 1954-2002. Chin Sci Bull 48:1224–1228. https://doi.org/10.1360/csb2003-48-11-1224 **(Chinese)**

Zhu C, Wang B, Qian W (2008) Why do dust storms decrease in northern China concurrently with the recent global warming? Geophys Res Lett 35:L18702. https://doi.org/10.1029/2008gl034886

Zou XK, Zhai PM (2004) Relationship between vegetation coverage and spring dust storms over northern China. J Geophys Res Atmos 109:D03104. https://doi.org/10.1029/2003JD003913

Zuo ZY, Zhang RH, Wu BY, Rong XY (2012) Decadal variability in springtime snow over Eurasia: relation with circulation and possible influence on spring time rainfall over China. Int J Climatol 32:1336–1345. https://doi.org/10.1002/joc.2355